EXPANDING THE OPERATIONAL ENVELOPE OF COMPACT CYLINDRICAL CYCLONE GAS/LIQUID SEPARATORS USING A VARIABLE INLET-SLOT CONFIGURATION

A Thesis

by

IGHOFASAN UVWO

Submitted to the Office of Graduate Studies of
Texas A&M University
in partial fulfillment of the requirements for the degree of

MASTER OF SCIENCE

December 2004

Major Subject: Petroleum Engineering

EXPANDING THE OPERATIONAL ENVELOPE OF COMPACT CYLINDRICAL CYCLONE GAS/LIQUID SEPARATORS USING A VARIABLE INLET-SLOT CONFIGURATION

A Thesis

by

IGHOFASAN UVWO

Submitted to Texas A&M University
in partial fulfillment of the requirements
for the degree of

MASTER OF SCIENCE

Approved as to style and content by:

Stuart L. Scott (Chair of Committee)	W. John Lee (Member)
Yassin Hassan (Member)	
Stephen A. Holditch (Head of Department)	

December 2004

Major Subject: Petroleum Engineering

ABSTRACT

Expanding the Operational Envelope of Compact Cylindrical Cyclone Gas/Liquid Separators Using a Variable Inlet-Slot Configuration.

(December 2004)

Ighofasan Uvwo, B.Eng., Russian State Oil and Gas University, Moscow, Russia

Chair of Advisory Committee: Dr. Stuart L. Scott

Despite the numerous advantages associated with using compact cylindrical cyclone gas/liquid separators, particularly for upstream production operations, the lack of a full understanding of the complex hydrodynamic process taking place in it and its “unfamiliarity” to oil field personnel has hindered its widespread use. The complexity associated with this technology is attributed to two limiting physical phenomena, liquid carry-over and gas carry-under. While a lot of work has been done to better understand and predict the liquid carry-over operational envelope, little or no information about methods capable of adequately predicting or characterizing the gas carry-under performance of such separators is available.

Traditionally, to mitigate the gas carry-under phenomena, the use of complex control algorithms and systems has been employed. These systems make the technology expensive (as opposed to the potential cost reduction it promises) and impractical for realistic use in the oil field where reliability is of critical importance.

A simpler solution, the use of changeable or adjustable inlet-slots that regulate the artificial gravity environment created in the separator, could significantly improve the gas carry-under performance of cylindrical cyclone separators.

This research has focused primarily on the use of adjustable inlet-slots. Theoretical analysis and experimental data investigating the benefits of variable inlet geometry have been provided. This work lays the foundation or validation required to perform more tests on a field-scale version to verify the results presented here. A modular design of such a variable inlet-slot inlet-section has the potential of simplifying the design and specifications of cylindrical cyclone gas/liquid separators.

From the results of this investigation, it was found that the gas carry-under performance of a cylindrical cyclone gas/liquid separator could be improved considerably over a wider range of operating conditions by adjusting the size of the inlet-slots. This contradicts earlier reports of liquid carry-over improvement in separator performance.

Also, for the first time, a simple method for theoretically analyzing the percent improvement in separator gas carry-under performance using the optimum g-force concept is presented. This method could be incorporated into design software for determining the slot-size configuration required for varying separator-operating conditions.

DEDICATION

I dedicate this work to my parents – Mr. & Mrs. Uvwo, all my brothers and sisters, teachers here at A&M, and my buddies.

ACKNOWLEDGMENTS

My biggest “thank you” goes to my graduate advisor Dr. Stuart Scott for his tremendous support, advice, and academic guidance.

My sincere appreciation goes to the members of my graduate committee, Dr. John Lee, and Dr. Yassin Hassan, for their scrutiny of, and contributions to, this research.

I couldn’t possibly or adequately express my gratitude to all the members of TAMU Multiphase Research Group for their constructive discussions, time, and effort during the course of this research.

To all my friends, I say a big thank you for making my stay at Texas A&M University worthwhile, memorable and a once-in-a-lifetime experience.

TABLE OF CONTENTS

CHAPTER Page

I INTRODUCTION 1

1.1 Background 1
1.2 Literature review 2
1.3 Objectives of the study 4
1.4 Thesis outline 5

II CONFIGURATION, APPLICATIONS AND OPERATIONAL CHARACTERISTICS OF CCGL SEPARATORS 6

2.1 Configuration of a cylindrical cyclone gas/liquid separator 6
2.2 Uses and applications 7
2.3 Operational characteristics of CCGL separators 10
2.3.1 Liquid carry-over (LCO) 10
2.3.2 Gas carry-under (GCU) 11

III EXPERIMENTAL FACILITY 13

3.1 Separator configuration 13
3.1.1 Test section 13
3.1.2 Novel inlet-section design with variable (changeable) inlet-slots 16
3.2 Instrumentation and data acquisition 16
3.3 Experimental procedure 16

IV INFLUENCE OF VARIABLE INLET-SLOT ON SEPARATOR PERFORMANCE 19

4.1 Zero-net liquid flow (ZNLF) 19
4.2 Effect of recombination points on separator performance 21
4.2.1 ZNLF holdup 21
4.2.2 LCO operational envelope 22
4.3 Liquid carry-over performance 24
4.4 Gas carry-under performance 27

V GAS CARRY-UNDER OPERATIONAL ENVELOPE EXPANSION 28

5.1 Theoretical analysis of CCGL separator GCU operational envelope expansion 28
5.2 Experimental validation of improved GCU performance 34
5.2.1 Assumptions in acquiring data 34
5.2.2 Factors influencing rate of GCU 35
5.2.3 Improved GCU performance using step-wise change of inlet-slot size 41

CHAPTER Page

VI CONCLUSIONS AND RECOMMENDATIONS 44

6.1 Conclusions 44
6.2 Recommendations 44

NOMENCLATURE 46

REFERENCES 48

APPENDIX A. PERCENT GAS CARRY-UNDER EVALUATION ALGORITHM. 51

APPENDIX B. EXPERIMENTAL DATA SET. 52

APPENDIX C. CGL SEPARATOR TEST SECTION. 62

VITA 64

LIST OF FIGURES

Page

Fig. 2.1 Basic operational configuration of a CCGL separator 6

Fig. 2.2 CCGL separator in a multiphase metering loop configuration 8

Fig. 2.3 Largest CCGL multiphase metering installation in the world. Depolyed by Caltex Indonesia. Physical dimensions: 5 ft. ID, 20 ft tall; rated at 200,000 bopd, 71 MMscfd, 170 psi and 360 ^{o}F. (From Marrelli and Kouba[17]) 9

Fig. 2.4 Operational envelope for liquid carry-over 10

Fig. 3.1 Schematic of CCGL separator test loop 13

Fig. 3.2 Schematic of test section 14

Fig. 3.3 Schematic of the inlet-section and changeable inlet-spools (see Appendix C for more pictures) 15

Fig. 3.4 Data acquisition system 17

Fig. 4.1 ZNLF holdup profile for different slot configurations 21

Fig. 4.2 ZNLF holdup profile for three different recombination points 22

Fig. 4.3 LCO operational envelope profiles for recombinations # 1-3 23

Fig. 4.4 LCO operational envelope at 3 and 6 psi 24

Fig. 4.5 LCO opereational envelope at 9 psi 25

Fig. 4.6 LCO operational envelope at various separator operating pressures 26

Fig. 5.1 CCGL separator ID as a function of gas production rate and operating pressure 31

Fig. 5.2 Lines of constant g's required for efficient separation 32

Fig. 5.3 Lines of constant inlet-slot cross-sectional area (expressed as equivalent diameter - d_{inlet}) 33

Fig. 5.4 Separator operating pressure profiles for slot #1-3 36

Fig. 5.5 Variation of percent gas carry-under of inlet stream with g-force of separation for slot #3. 37

Page

Fig. 5.6 Percent GCU trend for slot #3 38

Fig. 5.7 g-force trend for slot #3 38

Fig. 5.8 Percent GCU trend for slot #2 39

Fig. 5.9 g-force trend for slot #2 39

Fig. 5.10 Percent GCU trend for slot #1 40

Fig. 5.11 g-force trend for slot #1 40

Fig. 5.12 GCU performance of slots #1-3 at 250-lb/min water rate 42

Fig. 5.13 GCU performance of slots #1-3 at 200-lb/min water rate 43

LIST OF TABLES

Page

Table B.1 Zero-net liquid flow – slot #1-3 52

Table B.2 Zero-net liquid flow – slot #1 (recombinations #1-3) 53

Table B.3 LCO operational envelope 54

Table B.4 LCO operational envelope – separator pressure 55

Table B.5 GCU operational envelope – slot #1 (constant gas rate) 56

Table B.6 GCU operational envelope – slot #1 (constant liquid rate) 57

Table B.7 GCU operational envelope – slot #2 (constant gas rate) 58

Table B.8 GCU operational envelope – slot #2 (constant liquid rate) 59

Table B.9 GCU operational envelope – slot #3 (constant gas rate) 60

Table B.10 GCU operational envelope – slot #3 (constant liquid rate) 61

CHAPTER I
INTRODUCTION

1.1 Background

The use of compact separation technology, such as cylindrical cyclone gas/liquid separators, has been identified as a means of reducing expenses associated with production operations. Cylindrical cyclone gas/liquid (CCGL) separators, compared to the conventional vessel-type separators, are simple, compact, low-cost, low-weight, and are easy to maintain and install.

These advantages have been the major driving force promoting the use of CCGL separators in such applications as in multiphase metering loops[1] (portable well-testing and permanent metering loops), enhancement of the performance of multiphase pumps (by regulating/reducing the gas/liquid ratio), bulk-separation, flare gas scrubbing, downhole separation and even as primary separation of gas and oil/water mixtures.

To date, over 350 cylindrical cyclone gas/liquid separators have been installed and put to use for various applications[2]. Despite the advantages inherent with the use of CCGL separators, its efficient operation is limited by two major physical phenomena – gas carry-under (GCU) and liquid carry-over (LCO). While a lot of work has been done in understanding the complex hydrodynamic flow behavior in CCGL separators (particularly for LCO), thus enabling the formulation of necessary design criteria to minimize these phenomena, no significant attempts have been made to "tailor-fit" this novel technology for "practical" use.

Due to the very short retention time and the dynamics of the process conditions in which CCGL separators operate, the use of complex control-valves and algorithms has been ineffective and/or impractical. Also, installations today are equipped with a constant or fixed inlet-geometry thus restricting their application over a wide range of operating conditions. Expansion of the operational envelope, by means of variable inlet configuration is imperative if this technology is to compete viably with, or replace entirely, conventional vessel-type separators.

The expansion of the operational envelope of CCGL separators through the use of such a variable inlet configuration, coupled with some control has the potential of further driving down

---

This thesis follows the style and format of the *Journal of Petroleum Technology*.

the cost of CCGL separator units and even making “off-the-self” design of a compact cylindrical cyclone separator possible.

1.2 Literature review

Literature review on compact cyclone separators dates back to studies conducted on conical hydrocyclones for gas/oil separation while recent research efforts have focused on experimental data acquisition through laboratory tests of low-pressure units to field-scale test and design of high-pressure separators. These recent research efforts have been aimed at optimizing the design of CCGL separator units by understanding the separation mechanisms governing liquid carry-over and gas carry-under phenomena.

Review of past efforts at understanding the physical phenomena occurring in a CCGL separator shows that research has focused on these general areas;

- Determining the nature of the flow field in the separator (forced/induced vortex; axial, tangential and radial velocity distributions and fluid particle velocity decay)
- Hydrodynamic models for predicting parameters essential for proper design of CCGL separators (gas/liquid interface shape, equilibrium liquid level, pressure drops across various components and operational envelope)
- Active and passive control systems for regulating and monitoring separator performance

The research methods employed involved one or more of the following

- Experimental investigation
- Mechanistic modeling
- Simulations using various commercial computational fluid mechanics (CFD) codes

Millington and Thew[3] (1987) documented the existence of a forced vortex with a tangential velocity profile by using Local Laser Dopler Anemometer for velocity measurements. Based on the results of the experiments, they concluded that an important controlling factor of the rate of GCU was the distance between the tangential inlet into the separator and the outlet. Experiments conducted by Reydon and Gauvin[4] (1981) showed that the magnitude of the tangential inlet velocity does not change the shape of the tangential velocity, axial velocity and pressure profiles. Only an increase in their magnitudes occurs. Farchi (1990) conducted further tangential velocity measurements that supported Millington and Thews’ observation of the presence of a forced

vortex. Farchi noted, though, that this forced vortex structure decays into a free vortex profile with increasing cyclone diameter. He conducted his tests using static pitot tubes in a cylindrical cyclone separator. Recent research efforts using high-tech and fast CFD simulations have attempted to characterize the flow field in cylindrical cyclone separators. Bandyopadhyay *et al*[5] simulated the trajectory of a single gas bubble introduced in the flow stream inside a CCGL separator. Further flow field characterization combined with visualization experiments by Erdal *et al*[6] investigated the effect the gas-liquid interface has on the complex flow field below the inlet. Erdal simulated single- and two-phase flow and investigated the behavior of small gas bubbles in the lower part of cylindrical cyclone separators as related to gas carry-under.

With the objective of optimizing the design and predicting the performance of cylindrical cyclone gas/liquid separators, detailed mechanistic models have been built to characterize the hydrodynamics of the gas/liquid flow in such separators. Kouba *et al* (1995)[7] examined CCGL separator design and performance issues. He also presented first attempts to develop a mechanistic model for predicting gas carry-under[8]. The proposed model predicted the gas-liquid interface near the separator inlet that was used as the starting point for bubble trajectory analysis. Arpandi *et al* (1996)[9] developed a mechanistic model that enables prediction of the hydrodynamic flow behavior in a CCGL separator. This model predicts the LCO operational envelope, equilibrium liquid level, vortex shape and pressure drop across the separator. Another mechanistic model, developed by Chirinos *et al* (1999)[10], modeled the percent LCO beyond the operational envelope. This model was extended to high-pressure conditions. Gomez *et al* (2000)[11] enhanced previous mechanistic models by including a flow pattern dependent nozzle analysis. The proposed model was then used in designing four units for industrial application.

Control and operability of cylindrical cyclone separators over a wide range of operating conditions have also been addressed. Wang *et al*[2] proposed an optimal control strategy for adapting CCGL separators to gas and liquid flow rate fluctuations. Experimental investigation and mathematical simulation using Mathlab/Simulink were used. The physical control system consisted of liquid and gas control valves, pressure transducers and level position sensors. Isenberger[12] and Barbuceanu[1] investigated expanding the operational envelope of a compact cylindrical cyclone separator using a variable inlet design that could easily be altered to adapt to changing wells conditions. Barbuceanu's results indicated that this method could expand the operational envelope for LCO by as much as 300%.

Expanding the operational envelope of CCGL separators, particularly for gas carry-under, would significantly improve the performance of multiphase meters utilizing CCGL technology for partial separation. One of the major challenges in designing a CCGL separator for use in multiphase metering applications, as acknowledged by the relevant automation and process industry, has been the prevention or elimination of gas being carried along with the liquid stream[13]. Entrained gas reduces the accuracy of the conventional single-phase meters in these systems.

To date, several CCGLS-based multiphase meters have been deployed and tested on a field-scale basis. Kvaener Process Systems and Statoil developed a compact cyclone multiphase meter[14]. This unit, coupled with a microwave water-cut measurement, a coriolis flow and density measurement, and appropriate gas measurement, was used as a complete well testing system in oil fields in North and South America. Four other units of the Kvaener/Statoil multiphase meter replaced conventional two- and three-phase separators that could not handle the increased liquid and gas rates from the BP Milne Point Alaska[13]. Other authors have identified significant benefits of using CCGL separators for multiphase metering applications[15,16].

Potential benefits such as the ability to test and monitor individual well flowrates frequently (more than twice a month as is the practice now) will help improve reservoir management and optimize production (diagnosis of individual wells). For remote subsea wells, this would provide a higher level of monitoring than is currently available on conventional vessel type test separators. Issues with radioactive devices, present in other multiphase metering technologies can also be avoided. Overall, due to the simplicity of a CCGL multiphase metering configuration and operation (no moving parts and presence of conventional single-phase meters and water-cut analyzers), reliability and familiarity will be an added benefit.

The use of a variable inlet-slot configuration in regulating/optimizing gas carry-under performance of CCGL separators is a promising step towards harnessing the numerous benefits associated with using this technology in multiphase metering applications.

1.3 Objectives of the study

The objective of this study is to investigate the expansion of the operational envelope of a compact cylindrical cyclone gas/liquid separator using a new variable inlet-slot configuration.

The optimum operating conditions for each slot configuration will be determined. The results of this experimental investigation will be used to verify the theoretical analysis of the expanded operational capacity achievable by means of using the variable inlet-slots. This will form a documented basis for justifying the need to incorporate modular inlet-sections with variable tangential inlet-slot sizes that are adjustable to varying operating conditions (liquid and gas rates).

1.4 Thesis outline

Starting with an illustrative description of the cylindrical cyclone gas/liquid separator, its operating principle, and applications of the technology, the inherent limitations will be discussed, namely the onset of liquid carry-over and gas carry-under. Next will be a description of the experimental facility and procedure used for investigating the performance of the separator fitted with different inlet slot-sizes.

The effect of using a variable inlet-slot configuration on the overall performance of the CCGL separator is then reported for the different separator characteristics such as the zero-net liquid flow performance, recombination-point effect on separator performance, liquid carry-over and gas carry-under performance. Where possible, theoretical analysis of each result obtained is presented.

In conclusion, observations and recommendations are made based on the results of this investigation.

CHAPTER II
CONFIGURATION, APPLICATIONS AND OPERATIONAL CHARACTERISTICS OF CCGL SEPARATORS

2.1 Configuration of a cylindrical cyclone gas/liquid separator

A cylindrical cyclone gas/liquid separator consists simply of flanged lengths of pipes and a middle inlet-section for creating the artificial g-environment for separation of the gas and liquid phases. The various components are shown in Fig. 2.1. The inlet-section, the most critical part for the efficient operation of a CCGL separator, is located at the middle. Above this is the gas-leg and exit and below is the liquid-leg and exit.

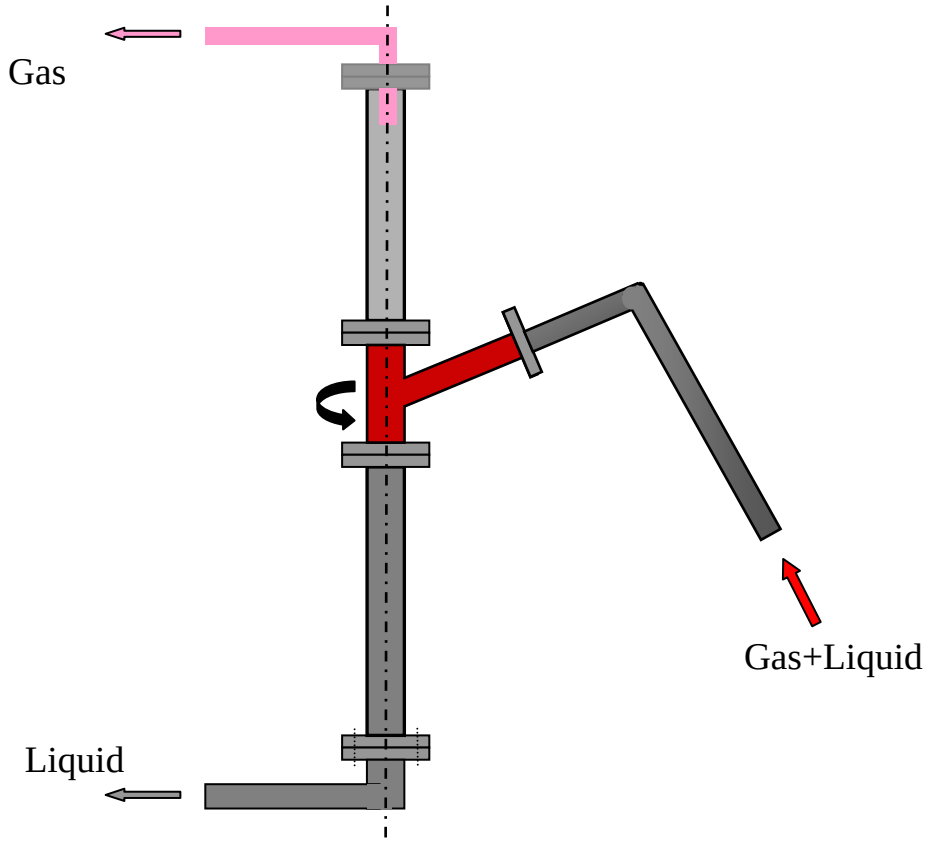

Fig. 2.1 Basic operational configuration of a CCGL separator

The inlet-section is a cylindrical pipe with an inclined tangential inlet. A multiphase mixture of oil, water, and gas entering is spun rapidly, impacting centrifugal force that facilitates the separation of the denser liquid phases from the gas stream. The liquid stream is thrown to the wall and, due to gravity, exits below through the liquid leg exit. Buoyancy forces move the gas phase to exit through the gas leg exit. From here onwards, depending on the application, the liquid and the gas stream can be recombined as in the case of a multiphase metering loop configuration or left fully/partially separated.

2.2 Uses and applications

CCGL separators have a wide-variety of uses and applications such as

- Stand alone bulk separators, or for expanding the capacity of existing vessel-type separators especially for offshore platform production facilities where space is at a premium
- Flare gas scrubbers
- Enhancement of the performance of multiphase pumps by regulating/reducing the gas volume fraction of the liquid stream
- Multiphase metering loops (portable well testing and permanent metering loops).

The most common application is as part of a multiphase metering loop. Using the partial separation concept, use of a CCGL separator offers a very cost-effective and practical solution to metering gas, oil and water from producing fields. In a multiphase metering loop configuration, the gas and liquid exits are recombined after metering the rates of the individual gas and liquid phases. Fig. 2.2 and Fig. 2.3 show multiphase metering applications of CCGL technology.

The advantages associated with this configuration are:

- Improved accuracy of liquid measurement by concentrating the liquid phase
- Capability to self-regulate liquid level for small changes in flow conditions
- Use of conventional single phase meters for metering gas and liquid streams
- Absence of radioactive sources, usually present in conventional multiphase meters
- Overall simplicity of operation and maintenance (no moving parts) and low cost

However, despite the above-mentioned advantages, the effective operation of the CCGL separator is inhibited by two physical occurring phenomena – Liquid Carry-Over (LCO) and Gas Carry-Under (GCU).

Fig. 2.2 CCGL separator in a multiphase metering loop configuration (from Shen, Texas A&M Multiphase Metering User Roundtable, 2000)

Fig. 2.3 Largest CCGL multiphase metering installation in the world. Depolyed by Caltex Indonesia. Physical dimensions: 5 ft. ID, 20 ft tall; rated at 200,000 bopd, 71 MMscfd, 170 psi and 360 ^{o}F. (From Marrelli and Kouba[17])

2.3 Operational characteristics of CCGL separators

Due to the magnified g-forces applied to the fluid stream, CCGL separators require less residence times, hence their compactness. However, this short residence time and size available for separation of the gas and liquid phases, make them susceptible to foul operation whenever an upset in operating conditions occurs (slugging, abrupt changes in operating pressures and rates of bulk liquid and gas phases). To characterize this upset or reduction in separation efficiency, the terms liquid carry-over and gas carry-under are employed.

2.3.1 Liquid carry-over (LCO)

Liquid carry-over is defined as the onset of entrainment of the liquid phase in the gas stream exiting at the top of the separator. The set of all combinations of liquid and gas flow rates, or superficial velocities, below which LCO or GCU do not occur is defined as the operational envelope of a CCGL separator with respect to the respective phenomena. The superficial velocities, V_{SL} and V_{SG}, are defined with respect to the separator internal diameter, that is, the in-situ flowrate divided by separator cross-sectional area. In Fig. 2.4 is shown the typical shape of LCO operational envelope. The shape and size of the envelope for a particular separator is dependent on a variety of factors, the most important of which are the equilibrium liquid level in the separator, separator operating pressure, fluid viscosity, etc. It is (as will be shown later), however, independent on the size of the tangential inlet-slot (or spool) provided the geometry is obstruction-free to the flow of the entering multiphase mixture.

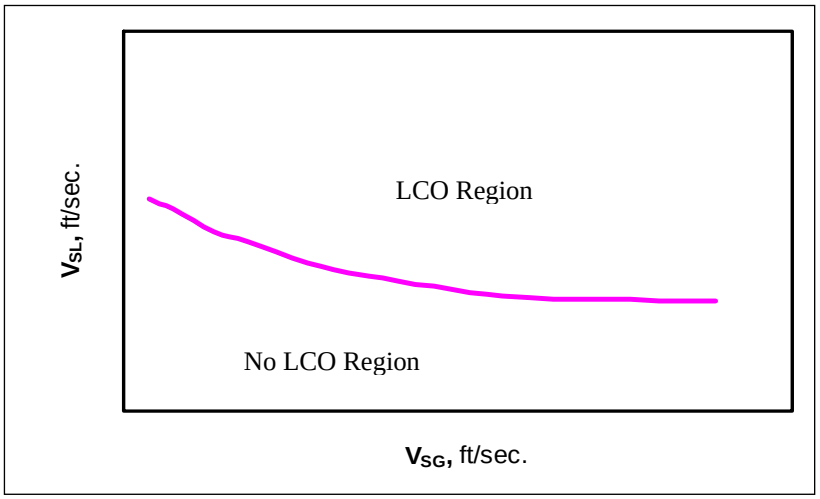

Fig. 2.4 Operational envelope for liquid carry-over

2.3.2 Gas carry-under (GCU)

Likewise, gas carry-under is the appearance of trapped gas bubbles in the liquid stream exiting from the bottom section of the separator through the liquid-leg exit. Amongst the factors affecting the occurrence of GCU are length of the liquid-leg (bottom section), magnitude of g-force impacted during separation, geometry of the inlet-section, and the nature of flow entering the inlet-section. A combination of any of these factors can lead to the initiation of GCU through one of the following mechanisms:

- Shallow radial trajectory of the individual gas bubbles which prevents the coalescence with the gas-core filament prior to exiting with the liquid stream into the liquid exit (case of insufficient design length of lower-section)
- Gas-core filament instability – helical whipping of the filament resulting into individual gas bubbles breaking-off into the liquid-leg exit (case of improper design geometry of inlet-section/tangential inlet or presence of obstruction in flow path of multiphase mixture during entrance)
- Bubble swarms as a result of sharp increases in liquid rate thereby producing a cloud of bubbles that escape coalescence with the central gas-core filament

It is the belief of the author, as confirmed by results of experimental data, that the most important factor influencing the initiation or rate of GCU is the magnitude of g-force impacted upon the multiphase mixture during entrance into a properly designed and operating CCGL separator. By "properly designed and operating" it is implied that the following conditions are satisfied:

- Gas-core filament instability (helical whipping) due to improper geometry is absent
- The equilibrium liquid level (ELL) during operation is just below the inlet of the multiphase mixture entering into the separator

Thus, for the efficient operation of a CCGL separator, a range of g-acceleration is required. To characterize the magnitude of the centrifugal force impacted upon separation, a dimensionless parameter – g's is used. The g's is obtained by dividing the centrifugal acceleration by the acceleration due to gravity. Typically, g's in the range of 50 to 100, for efficient CCGLS performance, is recommended. With this said, it is evident that application of CCGL separators over a wide-range of operating conditions is difficult or almost impossible to achieve with a fixed inlet-slot configuration. To cover a wider-range of liquid and gas rates, a means by which to regulate the g's is necessary if efficient operation is to be achieved. The use

of a variable inlet-slot configuration makes this achievable. And this has been the primary focus of this work at attempting to expand the operational envelope of a CCGL separator.

CHAPTER III
EXPERIMENTAL FACILITY

3.1 Separator configuration

3.1.1 Test section

The separator configuration used in this work is that of a multiphase metering loop. Fig. 3.1 shows the experimental setup of the CCGL separator used in this research.

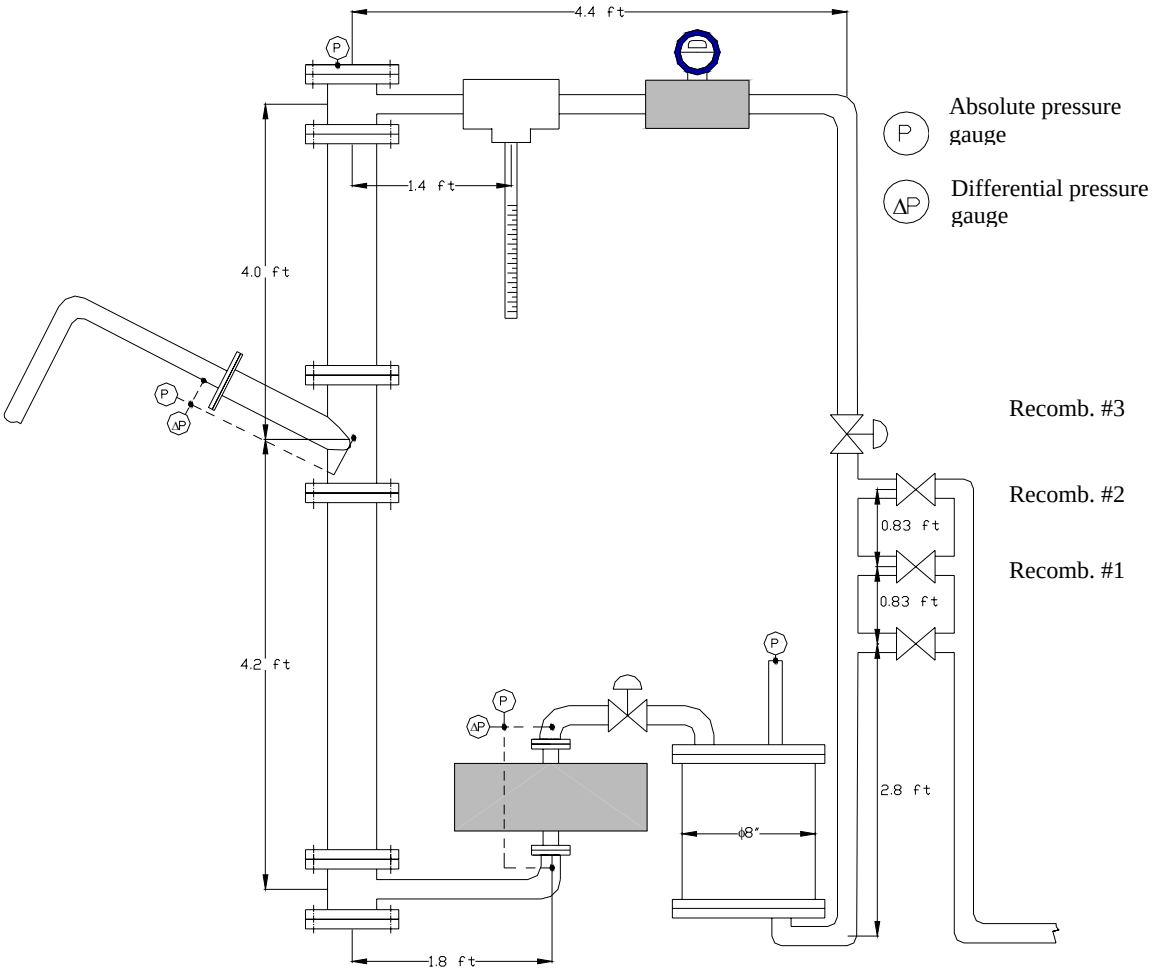

Fig. 3.1 Schematic of CCGL separator test loop

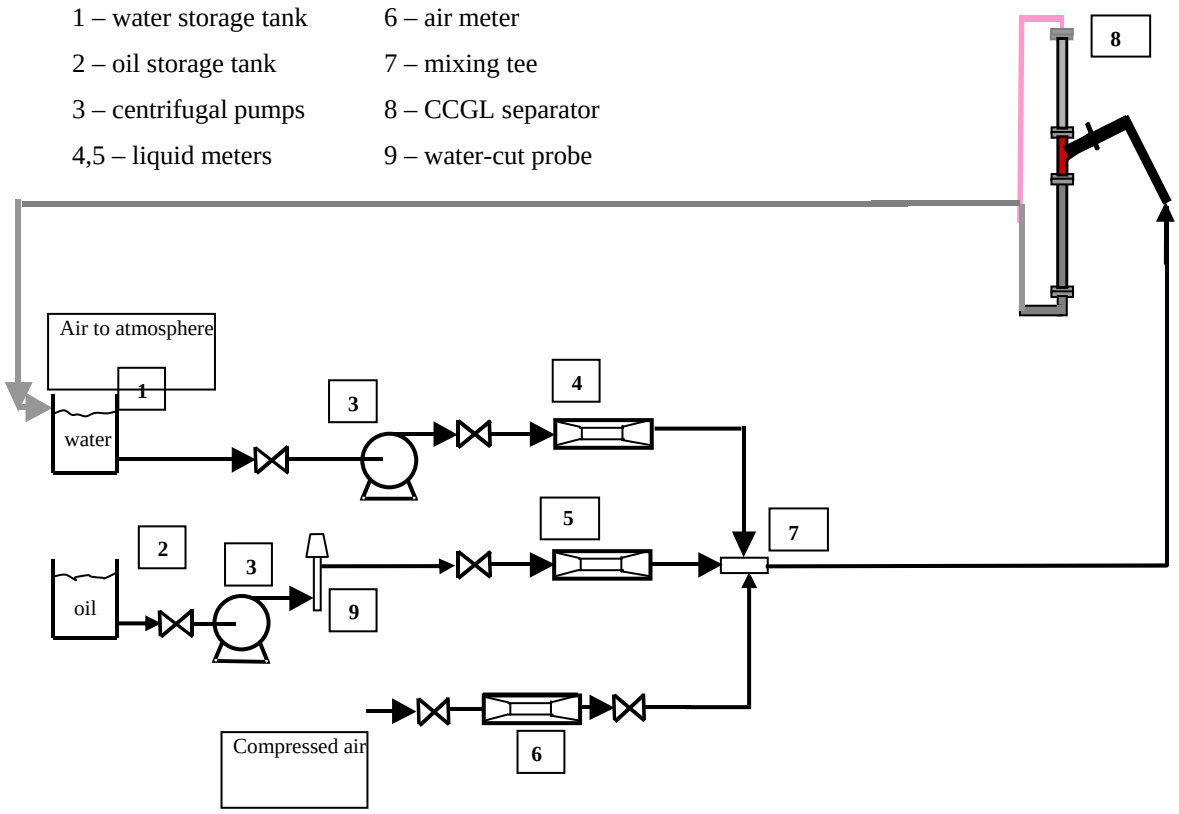

Fig. 3.2 Schematic of test section

The facility used for investigating improvements in the separator performance by means of the changeable inlet-spools is represented above in Fig. 3.2. The flow loop was run with air and water only. Water was supplied from a water storage tank ***(1)*** by a combination of two centrifugal and one progressive cavity pumps ***(3)***. Variable frequency drives were used for controlling liquid rates. Air supply for the gas loop was from a compressor and was regulated with a needle control valve. Gas flow rates were metered using an Elite Series Micromotion ½" coriolis meter ***(6)***, while water rates were obtained using a 1 ½" Model D Micromotion meter ***(4)***. Absolute and differential pressure transducers record various pressure data. The oil storage tank ***(2)***, pump ***(3)*** and meter ***(5)*** were not used in this work.

The air and water streams are combined at a mixing tee ***(7)*** and then onwards to the CCGL separator ***(8)***. From the separator, the two-phase mixture is directed back into the water storage tank where the air is vented to the atmosphere.

The 3-inch ID acrylic CCGL separator (Fig. 3.1) is equipped with a liquid trap at the gas-leg for detecting the onset of LCO. Also included is a 1-inch vortex-shedding meter for gas rate measurements of the separated gas phase. For a qualitative measure of the GCU rate, a gas-trap made out of an 8-inch PVC plastic tube was utilized. It is located downstream of the 1-inch coriolis meter. In this investigation, the vortex-shedding and coriolis meter were not utilized, although they were present in the configuration of the separator. The separated gas and liquid phases are recombined at the recombination points #1-3. A 12-inch tall inlet-section with a tangential inlet, inclined at 27^{o} from the horizontal, joins the gas- and liquid-leg.

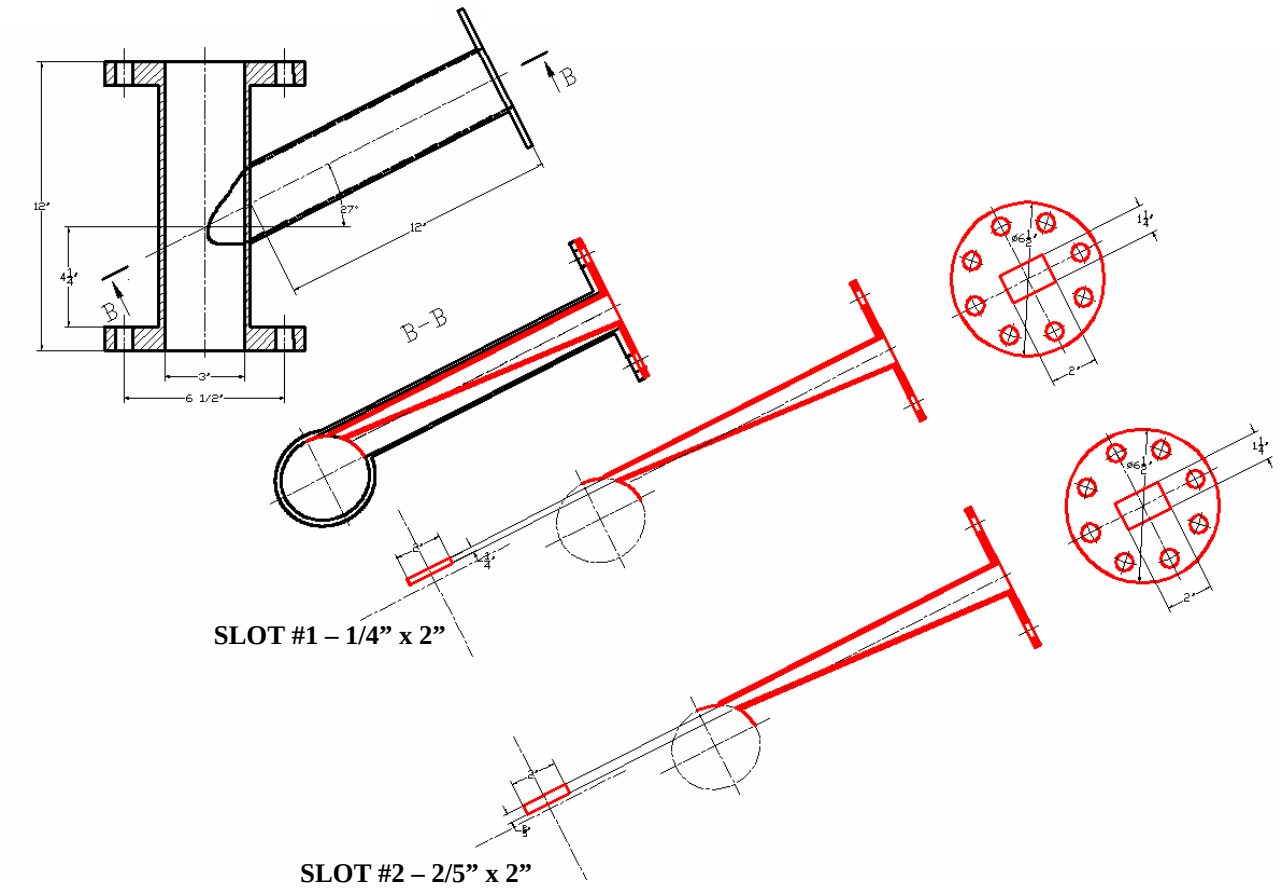

Fig. 3.3 Schematic of the inlet-section and changeable inlet-spools (see Appendix C for more pictures)

3.1.2 Novel inlet-section design with variable (changeable) inlet-slots

Fig. 3.3 shows the design schematic of the inlet-spools used in this investigation with two inlet-spools with rectangular slot areas of 0.00434 ft^2 (#1), and 0.00694 ft^2 (#2). The third slot used was the tangential inlet into the inlet-section without any inlet spool with an area of 0.03342 ft^2 (#3). Important design considerations were to:

1. Ensure smooth-surface contact of inlet-spool tip with the inner circumference of the inlet-section main body to prevent unnecessary turbulence generation.
2. Ensure almost tangential entry of the fluid stream into the separator for the benefit of optimal g-force generation at lowest mixture velocities.

3.2 Instrumentation and data acquisition

Signals from all measuring devices (pressure, flow rate, temperature and density) are acquired and recorded using a dedicated NI-DAQ data-acquisition system with LabView 6.0 as the GUI (see Fig. 3.4). All readings are acquired after suitable steady-state operating conditions have been reached. A 30-second, 2-Hertz acquisition for each data-point was employed.

3.3 Experimental procedure

To investigate, or characterize, the operational envelope improvement achievable by the use of a variable inlet-slot configuration tests on zero-net liquid flow, LCO and GCU were performed. The influence of recombining the gas and water at the various recombination points were also investigated.

For ZNLF tests, the liquid-leg exit is completely shut and then the CCGL separator is filled to the gas outlet with water. At this point, all liquid through-put through the separator is zero. Gas is then flowed through the stagnant liquid column until equilibrium is reached (liquid phase only churning with practically no liquid carry-over). At this point, the gas rate is recorded, and then gas flow is shut-off to record the equilibrium column of liquid left in the separator. This is repeated for different gas rates until total liquid blowout is achieved. This process was repeated for each inlet-spool configuration and for each recombination point.

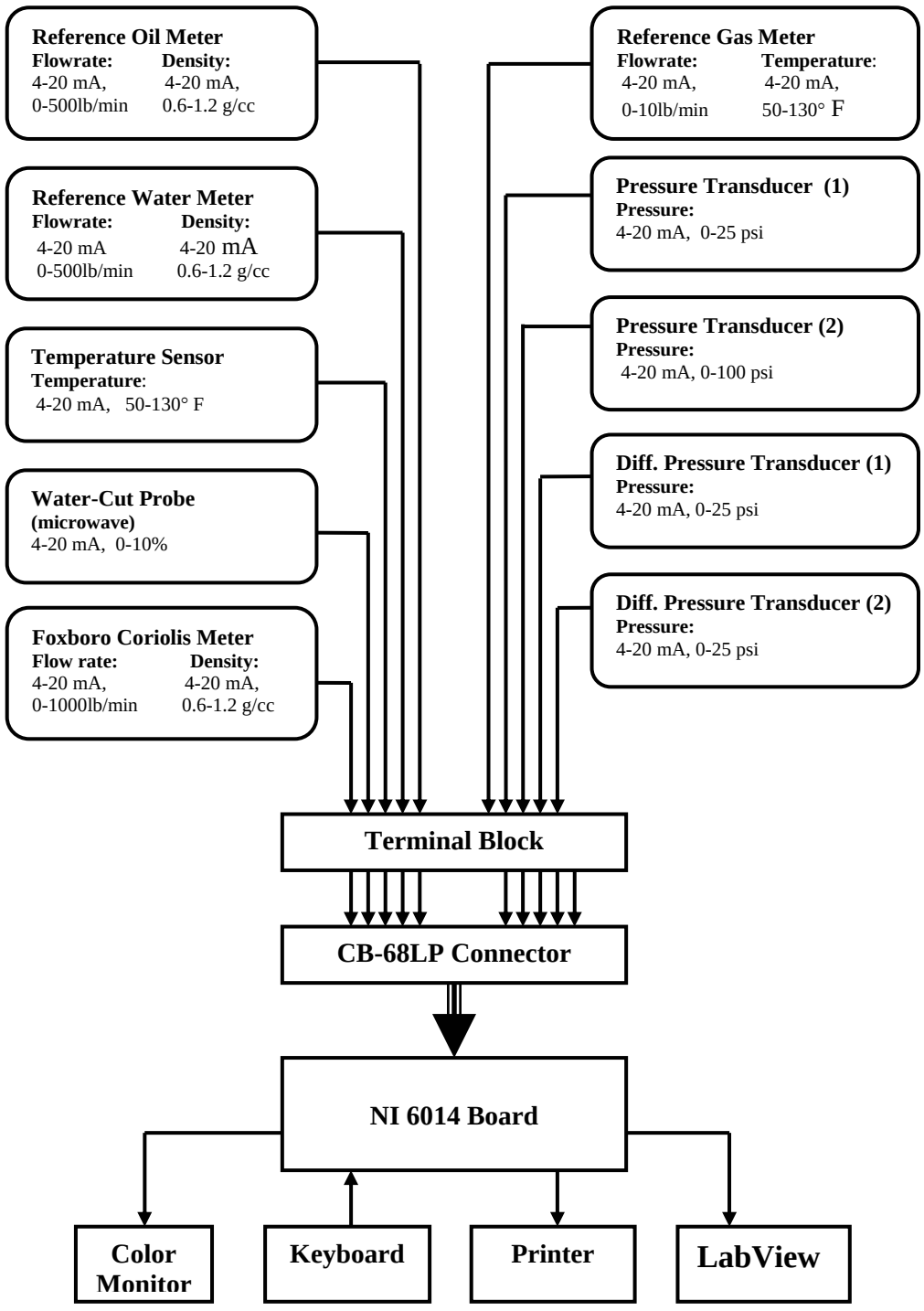

Fig. 3.4 Data acquisition system

LCO tests for each inlet-spool configuration were performed at constant separator pressures – 3, 6, and 9 psi. To define the LCO operational envelope, air mass rate is set at a constant value; liquid rate is then gradually increased until the onset of LCO is attained. Meanwhile, the control valve on the gas-leg exit of the separator is constantly readjusted until the desired pressure and liquid rate is achieved. This is then repeated for other gas rate until the whole operational envelope is covered as permitted by compressor and pump capacity. Liquid level control by means of adjusting the liquid-leg control valve was not employed. The valve was left fully opened through out the whole process.

GCU rate measurements were acquired at constant liquid and gas rates for each data point. System pressure is regulated by means of the gas-leg control valve to ensure the equilibrium liquid level in the separator is just below the entry point into the inlet-section. This provides optimum GCU performance. The results of these investigations are presented in chapter four.

CHAPTER IV
INFLUENCE OF VARIABLE INLET-SLOT ON SEPARATOR PERFORMANCE

4.1 Zero-net liquid flow (ZNLF)

Zero-net liquid flow is an important operational characteristic of a CCGL separator. During operation, whenever the Equilibrium Liquid Level (ELL) is located above the inlet ZNLF phenomena is observed. During ZNLF gas simply slugs/churns through the liquid column without any liquid being carried over.

ZNLF liquid holdup is an important parameter for characterizing the LCO operational envelope for a CCGL separator. Various ZNLF holdup models have been proposed. Arpandi *et al.* presented a low-pressure ZNLF model that uses Taylor bubble rise velocity method to estimate liquid holdup during ZNLF conditions. A high-pressure model, representative of the pressures and rates peculiar to subsea separation and metering applications, was developed by Duncan and Scott[18] to account for high-pressure effects on ZNLF holdup.

The basic expression for ZNLF holdup, H_{L0} , can be derived from the definition of slip between the gas and liquid phases, v_S;

$$v_S = v_G - v_L = \frac{v_{SG}}{1-H_L} - \frac{v_{SL}}{H_L} \tag{4.1}$$

For ZNLF, the liquid velocity is zero, thus

$$v_{Go} = \frac{v_{SG}}{1-H_{LO}} \qquad \text{and finally,} \qquad H_{LO} = 1 - \frac{v_{SG}}{v_{Go}} \tag{4.2}$$

Since the investigation in this work was performed at low-pressure conditions, the low-pressure ZNLF holdup correlations will be discussed here.

Arpandi's detailed two-phase hydrodynamic model[5] for predicting the LCO operational envelope combines equilibrium liquid level predictions with ZNLF holdup correlations to define the LCO operational envelope. ELL in the separator is, to a large extent, dependent on the pressure drop balance between the liquid and gas legs of the separator. His ZNLF holdup (for churn/slug flow in the upper-section), H_{L0} , can be evaluated from

$$H_{LO} = \left[1 - \frac{v_{SG}}{v_{Go}}\right] \cdot \left(1 - \frac{L_d}{L_{gl}}\right) \tag{4.3}$$

Where, the term, $(1 - L_d/L_{gi})$, accounts for the fact that holdup exits only in the upper-part of the separator that is in slug/churn flow.

The ZNLF gas velocity, v_{Go} , is a function of Taylor bubble rise velocity, and is expressed as;

$$v_{Go} = C_0 v_{SG} + 0.35\sqrt{g d_{sep}\left(\frac{\rho_l - \rho_g}{\rho_l}\right)} \tag{4.4}$$

L_d , length of the droplet region, is estimated from

$$L_d = \frac{1}{\frac{2g_c}{{v_{SG}}^2} - \frac{C_d}{2}\left(\rho_g v_{SG}\right)^2 \cdot \frac{3}{32\rho_l \sigma g_c}} \tag{4.5}$$

Results of ZNLF holdup obtained for the three different slot configurations are presented in Fig. 4.1. This data was obtained with recombination at point #1. From the plots, changing the slot configuration has practically no influence on the ZNLF holdup. Theoretical analysis of Equations 4.3 – 4.5 validates this result. Thus, the g's of separation (inlet-slot configuration) does not influence the ZNLF holdup performance of the CCGL separator. This conclusion appears to remain valid as long as the length of the upper gas section, L_{gl} , is long enough for slug/churn flow regime to be established before LCO is initiated.

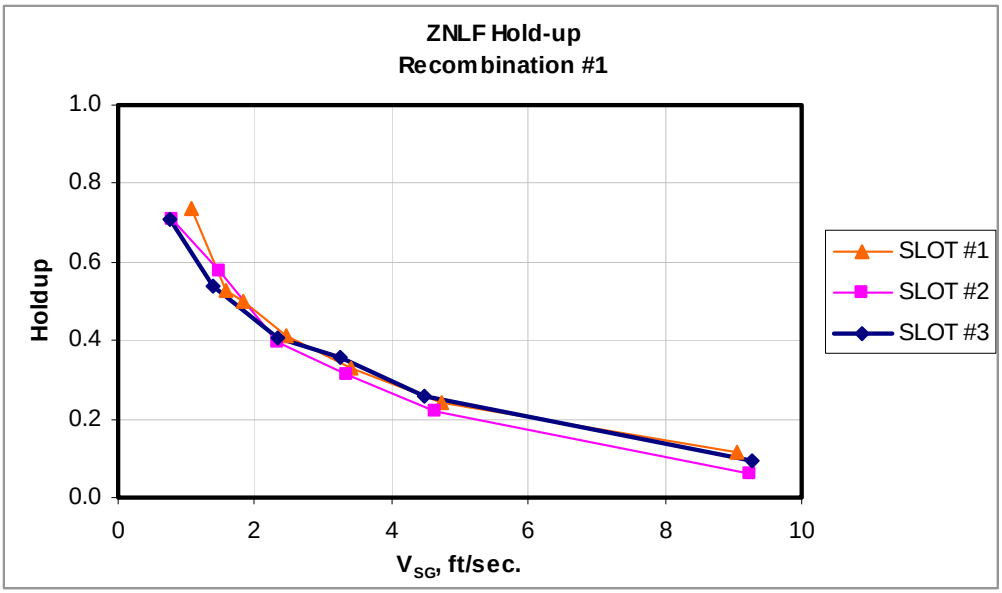

Fig. 4.1 ZNLF holdup profile for different slot configurations

Likewise, the point of recombination has no effect on the ZNLF holdup. This due to the fact that only the gas phase (air) is really flowing to an exit at atmospheric pressure. The recombination point effect on ZNLF holdup is presented in section 4.2.

4.2 Effect of recombination points on separator performance

4.2.1 ZNLF holdup

No difference in ZNLF holdup (see Fig. 4.2) is observed by varying the recombination point. During ZNLF, the system eventually comes to equilibrium (churning of liquid column above inlet of separator) with a fixed pressure – atmospheric at the outlet to which the air is vented.

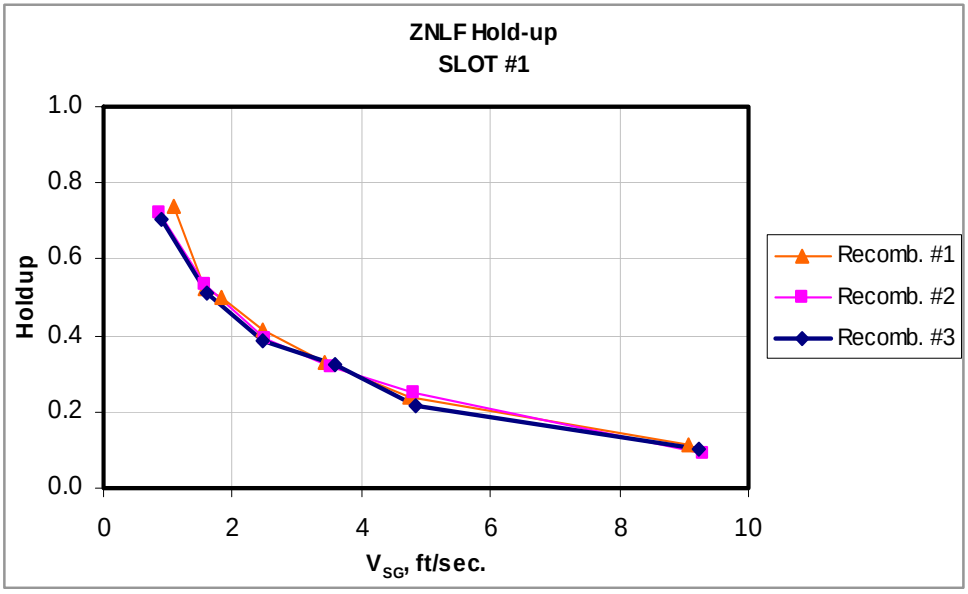

Fig. 4.2 ZNLF holdup profile for three different recombination points

4.2.2 LCO operational envelope

Significant improvement in LCO operational envelope is achievable by recombining the gas and liquid streams at the lowest point possible from the separator inlet. The plot in Fig. 4.3 shows clearly that an expanded LCO operational envelope is obtained at recombination #1 – the lowest location tested. Thus, it is important during the design of CCGL separators, for metering applications, to ensure the lowest possible recombination point to prevent premature LCO initiation.

Kouba *et al.*[7], by equating the pressure drop across the gas and liquid legs, expressed the ELL as;

$$L_{eq} = \frac{\sum F_L - \sum F_G + g\rho_l L_{l-recomb} - g\rho_g \left(L_{lH} + L_{gH} - L_{g-recomb}\right)}{g\cdot\left(\rho_l - \rho_g\right) - \left(\frac{\rho_l v_{lH}}{2}\cdot\frac{f_{lH}}{D_l}\right)} \qquad (4.6)$$

The effect of changing the recombination point (or height $L_{l\text{-}recomb}$) on the ELL, which ultimately determines the onset of LCO, can be analyzed by re-arranging Eq. 4.6 in the form

$$L_{eq} = \frac{\sum F_L - \sum F_G + g\left(\rho_l L_{l-recomb} + \rho_g L_{g-recomb}\right) - g\rho_g\left(L_{lH} + L_{gH}\right)}{g\cdot\left(\rho_l - \rho_g\right) - \left(\frac{\rho_l v_{lH}}{2}\cdot\frac{f_{lH}}{D_l}\right)} \qquad (4.7)$$

And, for a specific separator; $L_{l-recomb} + L_{g-recomb} = const$ (4.8)

At low pressure, the overall effect of increasing the recombination height, $L_{l\text{-}recomb}$ (thereby reducing the gas height $L_{g\text{-}recomb}$) with respect to the ELL will be increasing since the liquid density (ρ_l) is greater than the gas density (ρ_g) by several orders of magnitude. However, at higher pressure, it is expected that the operational envelope expansion as a result of lowering the recombination point would not be as significant.

The heights of the recombination points #1-3 from the liquid leg exit that were used in this investigation are;

Recombination #1: - 2.50 ft.

Recombination #2: - 3.39 ft.

Recombination #3: - 4.28 ft.

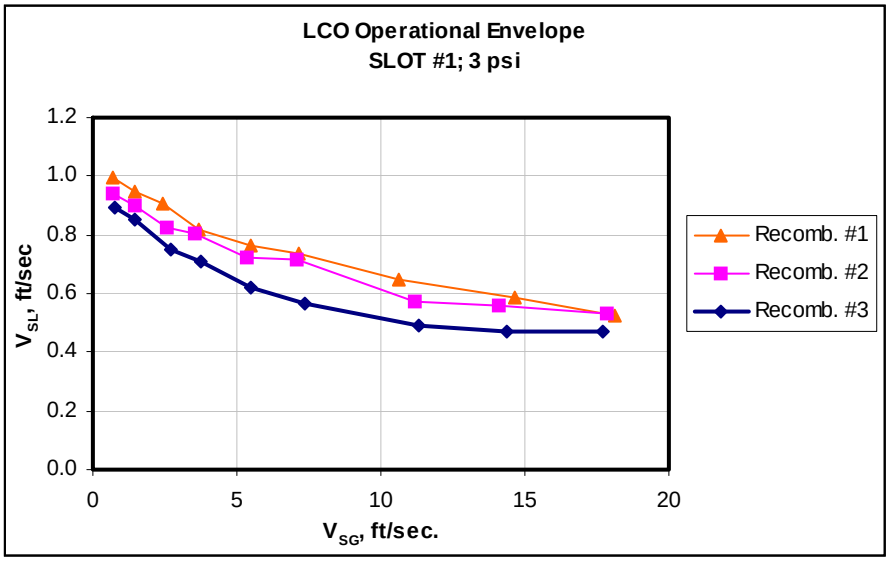

Fig. 4.3 LCO operational envelope profiles for recombinations # 1-3

4.3 Liquid carry-over performance

The variable slot configuration effect on LCO performance of the CCGL separator was investigated at three different separator pressures at recombination point #1. Interesting results, different from previous work that reported a considerable improvement in LCO performance, were obtained. LCO operational envelope results for slots #1-3 at the different separator pressures are presented in Figs. 4.4 and 4.5.

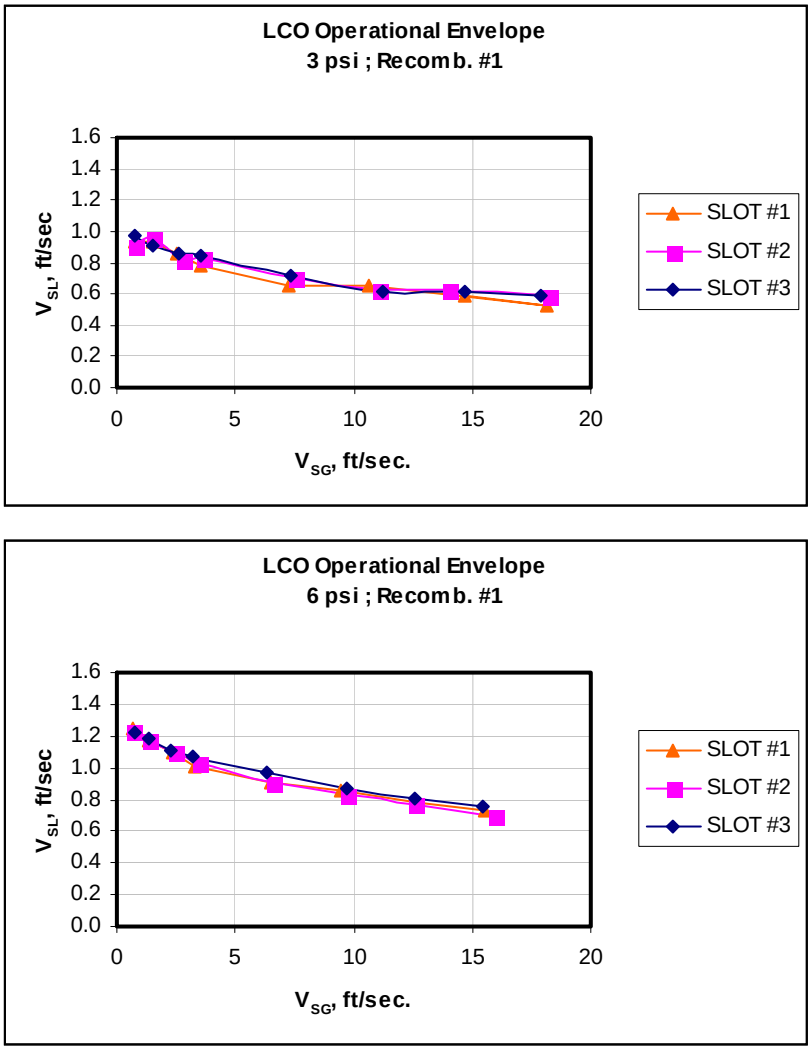

Fig. 4.4 LCO operational envelope at 3 and 6 psi

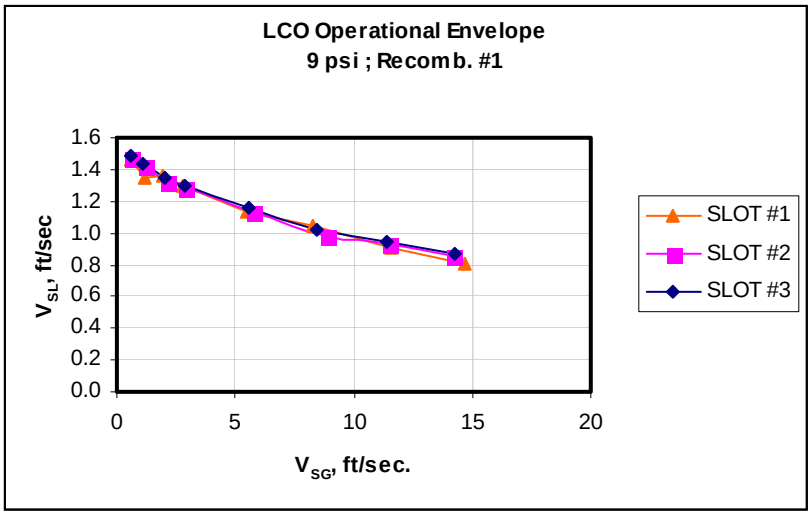

Fig. 4.5 LCO opereational envelope at 9 psi

These results show that the LCO operational envelope, at constant separator operating pressure, is not affected by the inlet-slot configuration. This once again, ascertains earlier statements that the LCO performance of the separator is primarily, determined by the pressure balance between the gas and liquid sections of the separator which translates into the ELL and the maximum liquid holdup, tolerable by the upper-section of the CCGL separator at a certain superficial gas velocity (see Eqs. 4.1 – 4.6).

Earlier reports of an improvement in LCO performance by means of changing the inlet-slot configuration, in my opinion, might have been due to gas expansion (different separator operating pressures during the experimental investigation).

However, the LCO performance is a strong function of separator operating pressure. Increasing separator pressure increases the operational envelope range. A comparison of the LCO operational envelope for each slot as a function of separator pressure is presented in Fig. 4.6. Higher separator pressure was obtained by choking back on the gas leg, thus effectively increasing the pressure drop across the gas leg. From the ELL correlation in Eq. 4.6, this would result in a lower ELL due to an increase in the total gas-leg frictional drop, ΣF_G , (liquid rate being constant). Thus for the initiation of LCO, the liquid rate has to increase to balance out the pressure drops in both legs.

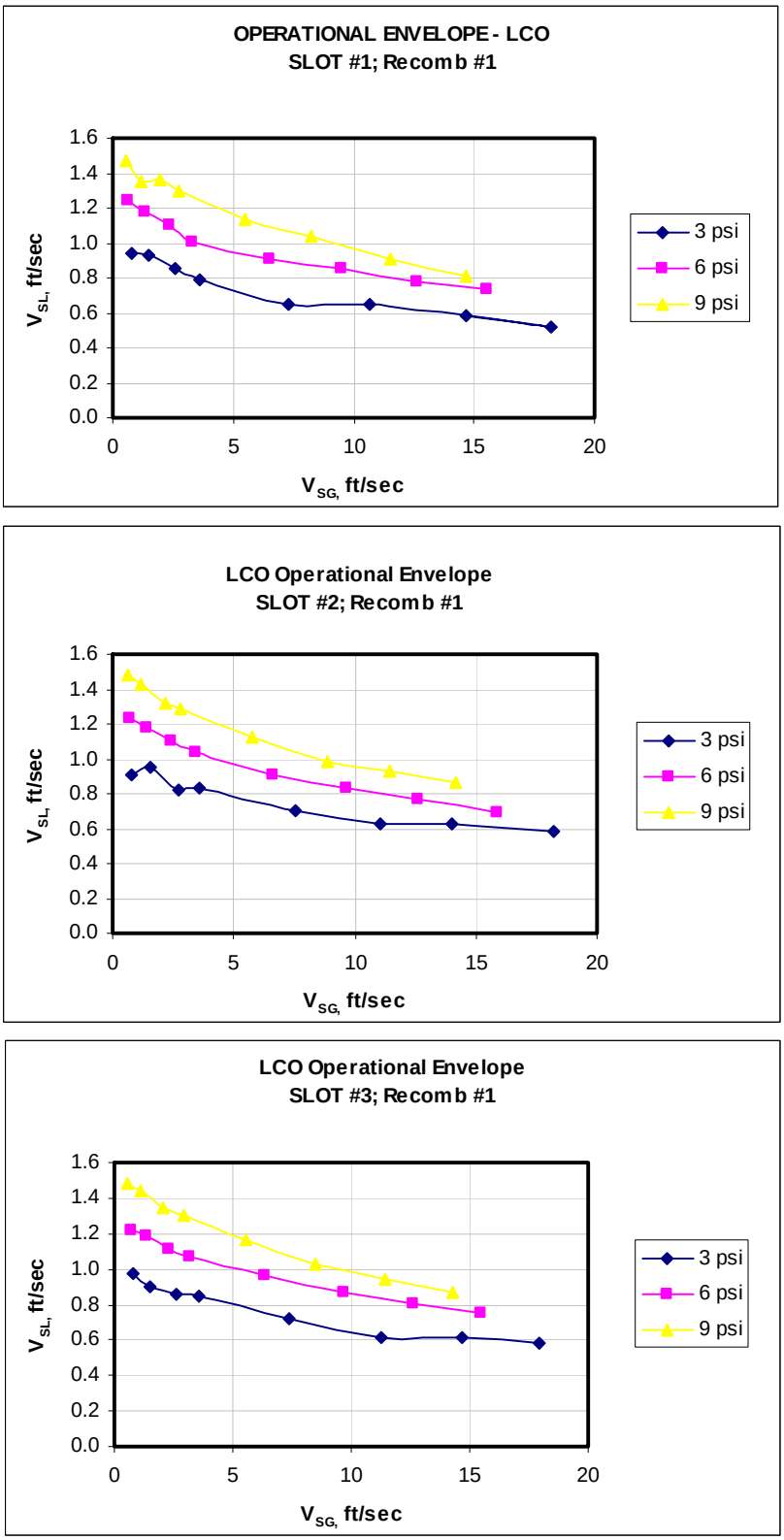

Fig. 4.6 LCO operatioanl envelope at various separator operating pressures

4.4 Gas carry-under performance

Observations during the LCO experiments showed that GCU initiated earlier with slot #3 and slot #2 than with slot #1, indicating that actual operational envelope expansion as a result of varying the inlet-slot configuration might be with the separator GCU performance. This was investigated and the results are presented in chapter V starting with a theoretical analysis of the potential operational envelope improvement achievable by changing the inlet-slot size.

CHAPTER V
GAS CARRY-UNDER OPERATIONAL ENVELOPE EXPANSION

5.1 Theoretical analysis of CCGL separator GCU operational envelope expansion

Since the use of g-force (in orders of magnitude greater than the acceleration due to gravity) is the main separation principle used in a CCGL separator, it makes physical sense to start the analysis from this perspective. Several authors[1, 19] have reported that g's in the order of 50-100 are required for the efficient operation of a CCGL separator. There is scarcely any actual experimental data confirming what range of g's provides efficient gas/liquid separation with consideration of fluid properties like foaming-tendencies[20-28]. From observations run with the air/water system in the lab, insufficient g's (less than 40) result in very poor GCU performance due to the absence of a defined gas-core filament to trap individual bubbles from exiting with the liquid stream. The plot on page 37 shows that the percent GCU-trends all approach zero asymptotically starting at about 40 g's. At excessive g's greater than 400 (on other plots on pages 39 and 40) for this system, the gas-core filament starts whipping and much finer gas bubbles are formed which are much easily carried-away with the liquid stream. In any case, a lower and upper range limit of g-force does exist for the efficient operation of CCGL separators. It is my opinion that for liquids with higher forming tendencies, the upper-range limit will be lower due to the greater probability of mixing (foam generation) rather than separating the two phases.

Having acknowledged the fact that a g-force boundary does exits, it is clear that for a wide-variety of flowing conditions, a CCGL separator fitted with a fixed-inlet will not operate optimally over a wide range. Thus, the necessity for a variable inlet-slot type configuration.

In this analysis, g's in the range of 50 and 100 will be used as an example.

The fundamental equation for quantifying the artificial gravity environment required to separate the gas/liquid mixture efficiently is in the form of g's, defined earlier as:

$$g's = \frac{v^2_{mr}}{g \cdot r_{sep}} \tag{5.1}$$

The radial component of the mixture entrance velocity, v_{mr}, is:

$$v_{mr} = \left(\frac{Q_l + k \cdot Q_g}{A_{inlet}} \right) \cdot \cos\alpha \qquad (5.2)$$

The factor, *k*, is a function of the physical properties of the gas and operating conditions (temperature and pressure). It evaluated from:

$$k = 0.02826 \cdot \frac{zT}{P} \qquad (5.3)$$

Substituting Eq. 5.2 into Eq. 5.1 and expressing the slot area required to obtain a specific *g's*-value in terms of other parameters will yield:

$$A_{inlet} = \sqrt{2} \cdot \cos\alpha \cdot \frac{Q_l + k \cdot Q_g}{\sqrt{g \cdot g's \cdot d_{sep}}} \qquad (5.4)$$

A simplified case scenario will be examined. The objective is to determine what inlet-slot area(s) will be required to meet the criteria – efficient operation of the CCGL separator within the 50 – 100 g's range. For this purpose, a producing well flowing at 3,000 Mscfd with total liquid production (oil) staying constant at 1,000 bopd is considered. Operating pressure and temperature of 120 psi and 90^{o}F respectively is assumed. As with any producing well, gas production declines with time to 700 Mscfd. Two cases considered are;

Case I considers a fixed-inlet configuration for the CCGL separator while Case II – a variable inlet-slot configuration. Case I represents the current trend in the design of compact cylindrical cyclone separators in operation today.

Sizing the CCGL separator internal diameter is done by evaluating a diameter above which liquid droplets of a nominal size (1000 microns used for this analysis) cannot be entrained by the exiting gas phase. This is achieved by equating the drag and buoyancy forces acting on this droplet size[18].

The derivation of the equation for evaluating this diameter is presented below.

The drag force, F_{drag} , acting on the liquid droplet is

$$F_{drag} = C_D \cdot A_{droplet} \cdot \left(\frac{V^2{}_t}{2 \cdot g} \right) \tag{5.5}$$

The buoyancy force, F_{bouy} , acting on the droplet is

$$F_{bouy} = \left(\rho_l - \rho_g \right) \cdot \frac{\pi \cdot D^3{}_{droplet}}{6} \tag{5.6}$$

The drag coefficient, is evaluated iteratively from

$$C_D = \frac{24}{\mathrm{Re}} + \frac{3}{\sqrt{\mathrm{Re}}} + 0.34 \qquad \text{and} \qquad \mathrm{Re} = 0.0049 \cdot \frac{\rho_g d_{droplet} V_t}{\mu_g} \tag{5.7}$$

Equating the drag and buoyancy forces, the terminal settling velocity for the droplet is expressed as (with necessary coefficients for oil field unit compatibility)

$$V_t = 0.0204 \cdot \left[\left(\frac{\rho_l - \rho_g}{\rho_g} \right) \cdot \frac{d_{droplet}}{C_D} \right]^{0.5} \tag{5.8}$$

The in-situ gas velocity is

$$V_{g\_insitu} = \frac{Q_{g\_insitu}}{A_{sep}} = 60 \cdot \frac{zT}{P} \cdot \frac{Q_g}{d_{sep}} \tag{5.9}$$

Finally, equating the terminal settling velocity to the in-situ gas velocity, the separator internal diameter yields:

$$d^2{}_{sep} = 5040 \cdot \frac{zTQ_g}{P} \cdot \left[\left(\frac{\rho_g}{\rho_l - \rho_g} \right) \cdot \frac{C_D}{d_{droplet}} \right]^{0.5} \tag{5.10}$$

In Fig. 5.1, change in CCGL separator diameter as a function of gas production rate is presented. The operating conditions are same as previously stated for the case scenarios discussed earlier. The effect of separator pressure on separator internal diameter is also shown.

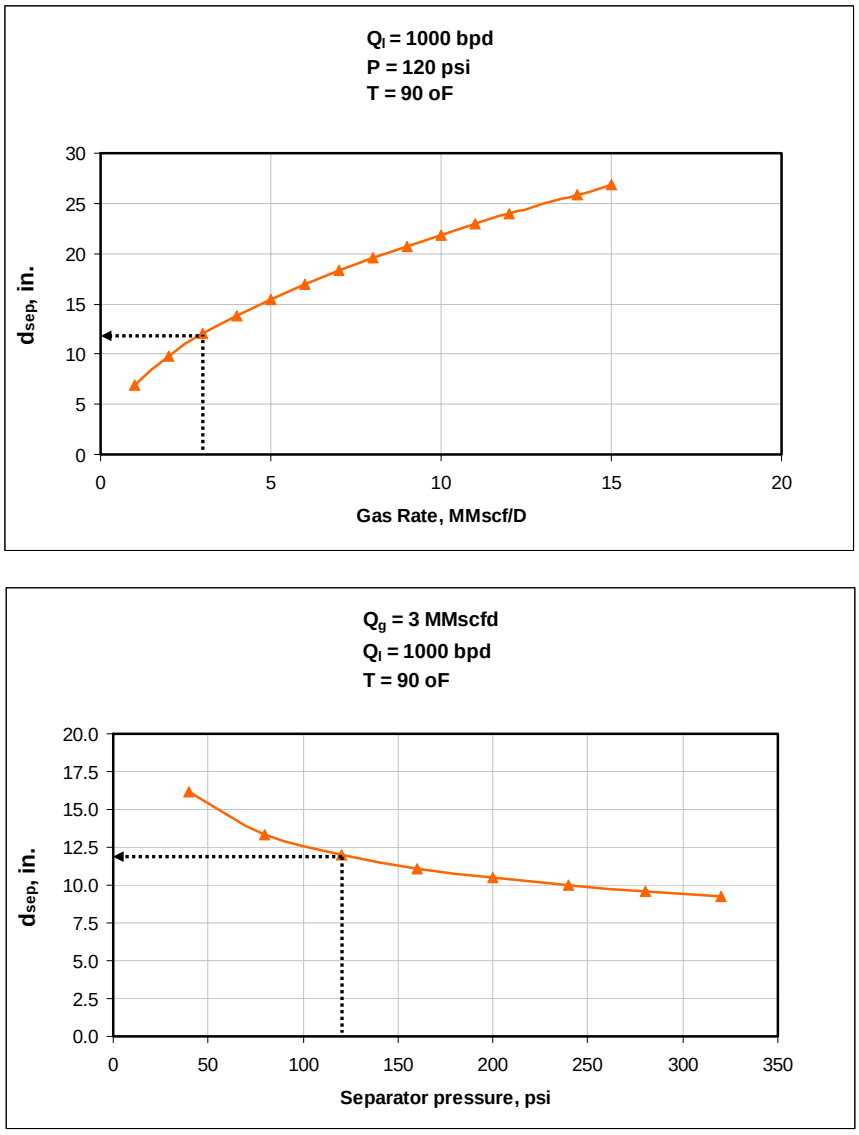

Fig. 5.1 CCGL separator ID as a function of gas production rate and operating pressure

From the plots above, a 12-inch ID CCGL separator will be required at 3 MMscfd. To better illustrate the relationship between the slot-size and g's, a plot of constant g's is presented in Fig. 5.2. Also, change in g's as a result of gas rate decline for specific slot-sizes, expressed as an equivalent circular diameter d_{inlet}, is presented in Fig. 5.3. It is assumed a separator with a fixed internal diameter is in operation.

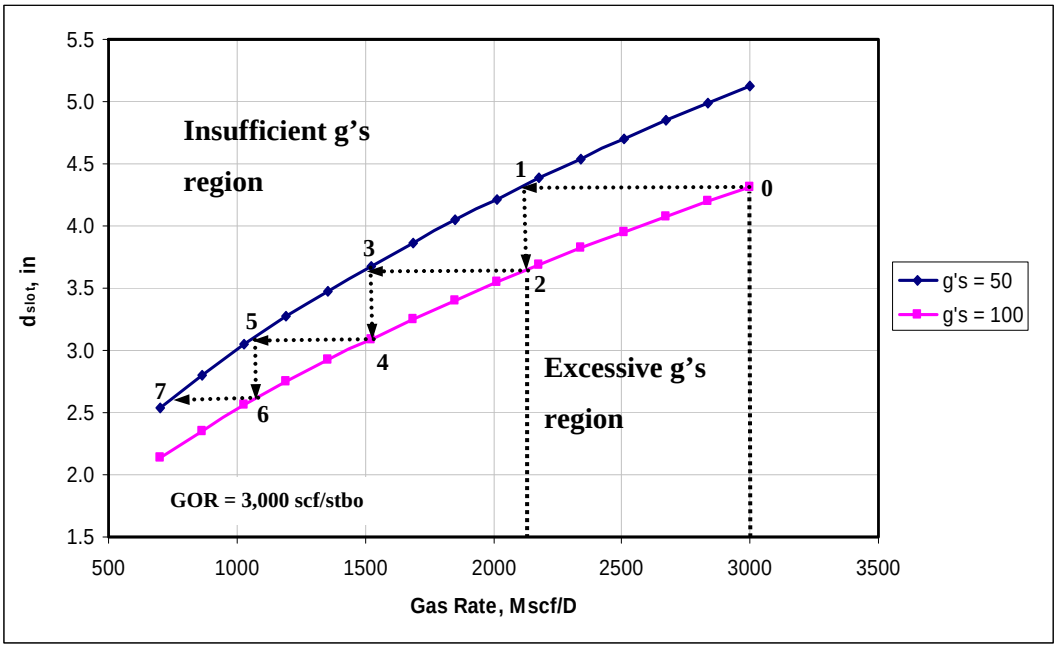

Fig. 5.2 Lines of constant g's required for efficient separation

The plots in Fig. 5.2 and 5.3 represent lines of constant ***g's*** and inlet cross-sectional area as a function of the daily gas production rate respectively. In Fig. 5.2, from Eq. 5.4, the inlet-diameters required to create a 50- and 100-g environment are shown. The region between these two lines represents the proper operating g-environment the separator should be in. Outside this region, to the right, excessive inlet-velocities will cause GCU (due to an elongated gas-core filament reaching the liquid exit or mixing rather than separation). To the left, insufficient g's prevent the formation of a gas-core filaments.

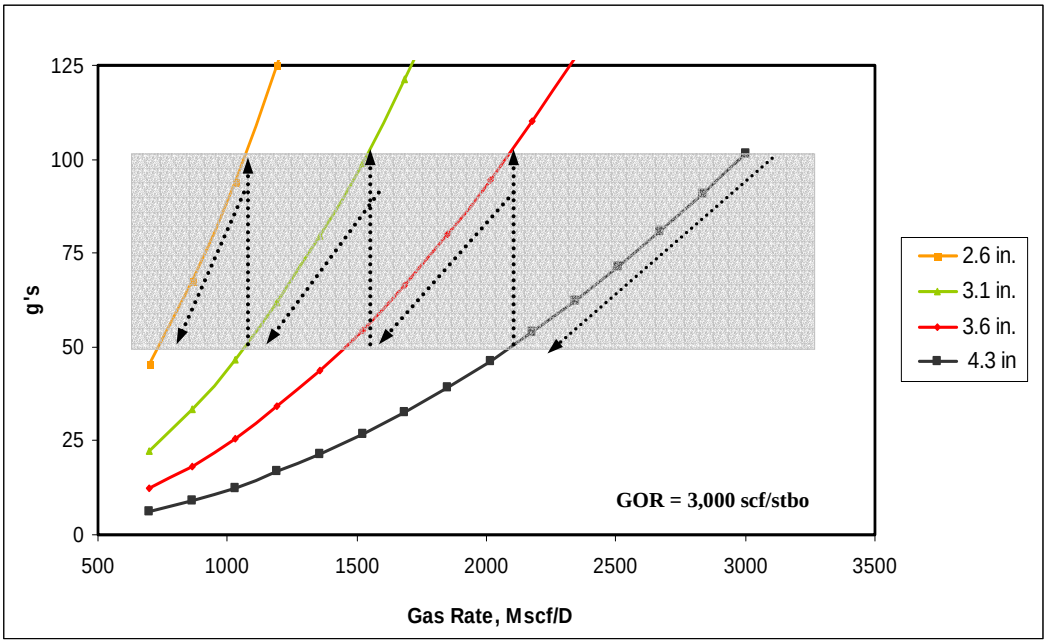

Fig. 5.3 Lines of constant inlet-slot cross-sectional area (expressed as equivalent diameter - d_{inlet})

In Fig. 5.3 the same information is presented, but in another form. Here, the decline in the g-environment at fixed inlet cross-sectional areas (expressed as $\boldsymbol{d_{inlet}}$) is displayed. The analysis begins with determining the inlet diameter for the maximum flow rate anticipated using a 100 g-environment. In this case, the equivalent circular diameter is 4.2 in. (see Fig. 5.3, trend 4.2 in). With decline in gas production, this value drops until a 50 g-environment is attained. Fig. 5.2 demonstrates this (line ***0-1***). In the case of a design with a fixed inlet-slot configuration (Case I) with a 4.2-in. inlet-slot equivalent diameter, decline of gas production rate below 2.1 MMscfd would force the separator into the "insufficient g-environment". Thus, for a CCGL separator with a fixed inlet-slot configuration, the operational range would be from 3.0 to 2.1 MMscfd - a span of 900 Mscfd.

For a CCGL separator with a variable inlet-slot configuration, as production declines below 2.1 MMscfd, a step-change of area ($\boldsymbol{d_{inlet}}$ from 4.2 in. to 3.6 in) is effected (line ***1 – 2***). This returns the separator to the 100-g environment. With further decline to about 1.5 MMscfd, another step-change to a 3.1-in. inlet-slot is necessary (line ***3 – 4***). This can be repeated until the

whole range for which the separator with the nominal diameter, d_{sep}, of 12 in. was designed for is covered.

Thus, the same separator fitted with a variable slot-type inlet can operate efficiently from 3.0 to 0.7 MMscfd – a span of 2.3 MMscfd. Comparing both cases, the variable-slot configuration of the separator can handle as much as 2.9 times the range of a fixed-slot type configuration.

In the next chapter, experimental data has been acquired and analyzed to verify the effect of using changeable insert-spools on the GCU performance of a CCGL separator. These tests show, qualitatively, that considerable expansion of separator GCU operational envelope is achievable with such a configuration.

5.2 Experimental validation of improved GCU performance

In trying to evaluate the GCU performance of the separator using the three slots (#1-3), a total of eighty-two data points were acquired. Gas carry-under rates were obtained by timing how long it took for entrained air bubbles to accumulate in the gas trap in Fig. 3.1. The gas trap is an 8-inch diameter and 19-inch tall vessel constructed from transparent PVC plastic. A 1-inch ID and 12-inch tall tube extends from the top for actual physical measurement of trapped-air volume, pressure and temperature. Gas rates of 0.22, 0.50, 0.75, 1.50, 3.00 and 5.00 lb/min and liquid rates of 150, 200, 250 and 300 lb/min were run. Separator operating pressure ranged from 3 – 20 psi.

5.2.1 Assumptions in acquiring data

The following assumptions were made on embarking on this investigation

- A qualitative analysis of the GCU was sought in this research. The gas trap trapping efficiency is far from 100%. Some bubbles escape with the liquid stream away from the trap-vessel. But, since the GCU performance of the slots are being compared at practically the same liquid and gas rates, as well as, same pressures, a qualitative comparison of their GCU performance is reasonable.
- Optimum GCU performance of each slot is being compared. This is achievable, as mentioned earlier in chapter II, by ensuring the ELL is just below the entrance of the tangential inlet into the separator. Lower ELL will result in more gas carry-under

because of insufficient travel-time for the gas bubbles to be drawn into the central gas-core filament. Higher ELL obstructs the upward free-flow of the gas trapped in the gas-core filament, thereby causing premature or increased GCU. Regulation of the adjustable valve on the gas leg is used for controlling the ELL. This also ensures the GCU performance of each slot is being compared at the same operating separator pressure. See Fig. 5.4 for the operating pressure profile for each slot.

5.2.2 Factors influencing rate of GCU

This section discusses some general trends observed from the data acquired on GCU performance.

5.2.2.1 Liquid rate influence on percent GCU

From the plots in Figs. 5.5 - 5.11 increasing liquid (water) flow rate results in higher percent GCU. This trend is the same for all the three slot configurations and at all g-force ranges investigated. This would mean that once GCU is initiated, further increase in liquid rates would aggravate the situation.

5.2.2.2 Effect of g's on GCU performance

Interesting trends of the influence of the magnitude of g forces on GCU performance are observed. For slot #3, the maximum g's attained within the flow rate range of this investigation is 110 (see Fig. 5.7). The trends for all liquid rates show a decline in percent GCU rate. At about 40 g's, the percent GCU rate of all trends in Fig. 5.6, approaches zero. This confirms that the lower range of the effective g's required for efficient separation of the tested system is about 40 – 60 g's.

The percent GCU trends for slot #1 and slot #2 behave differently. From Fig. 5.9 and 5.11, at about 400 – 600 g's the percent GCU rate starts to increase again. This qualitatively validates earlier statements of the existence of an upper-range value of g's. Quantitatively, what exact value this upper-range limit is cannot be estimated from this investigation due to the inefficiency of the gas-trap. The purpose of this GCU performance analysis was to compare the GCU performance of the three inlet-slots #1, #2 and #3 (see Figs 5.12 and 5.13) at the same operating process conditions of liquid and gas rates and pressure.

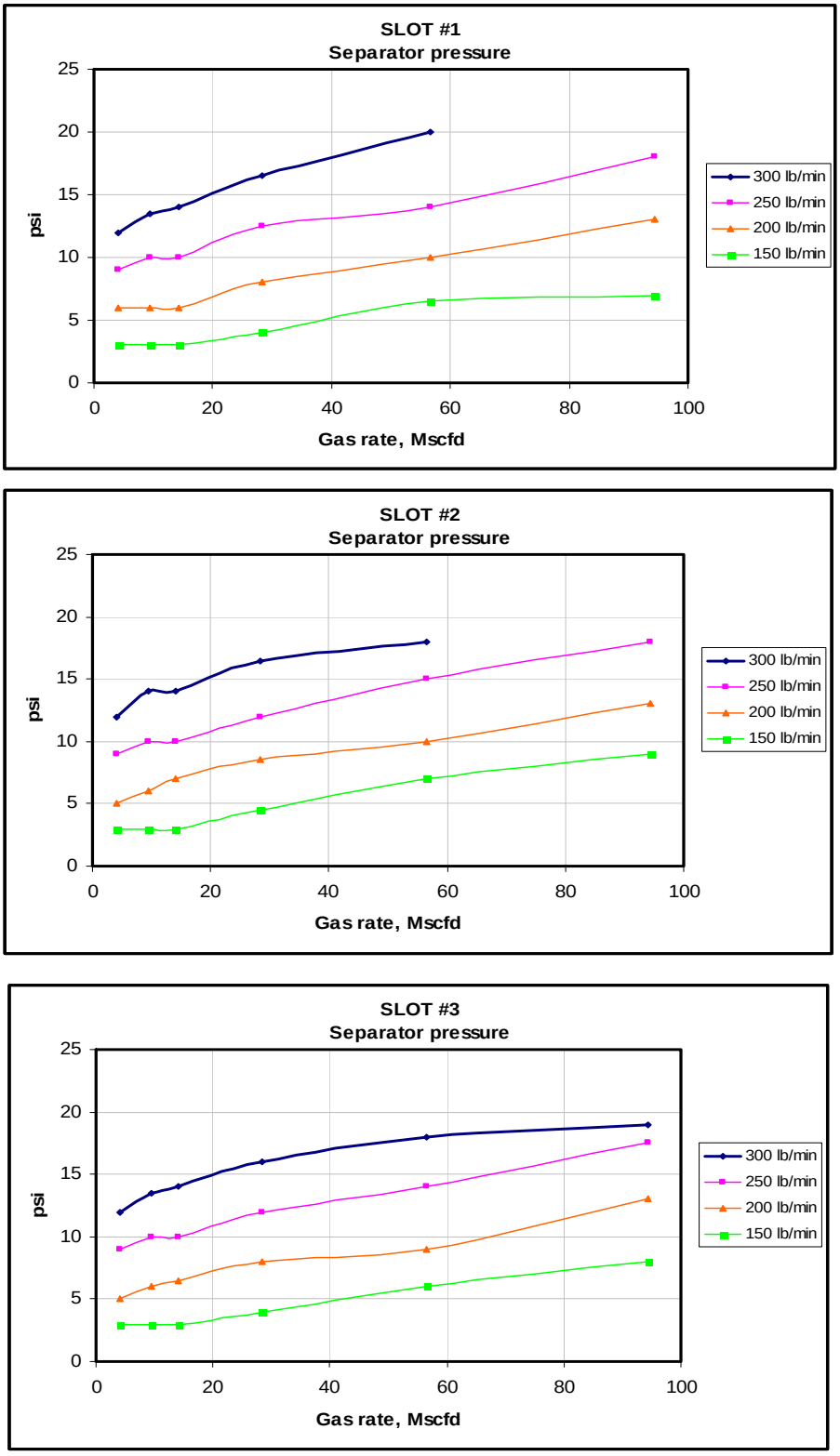

Fig. 5.4 Separator operating pressure profiles for slot #1-3

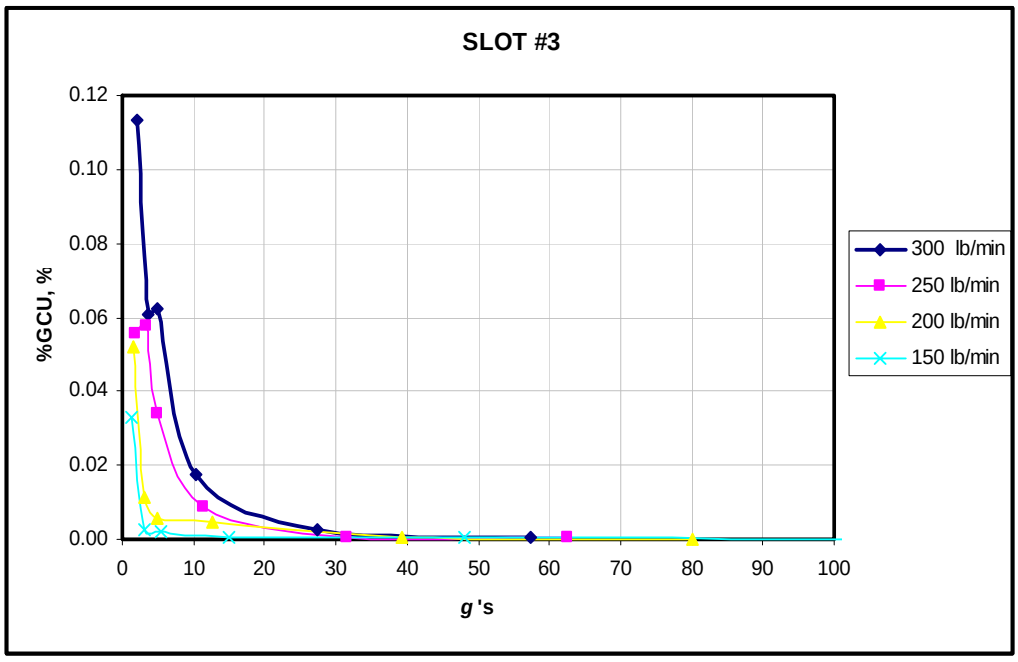

Fig. 5.5 Variation of percent gas carry-under of inlet stream with g-force of separation for slot #3

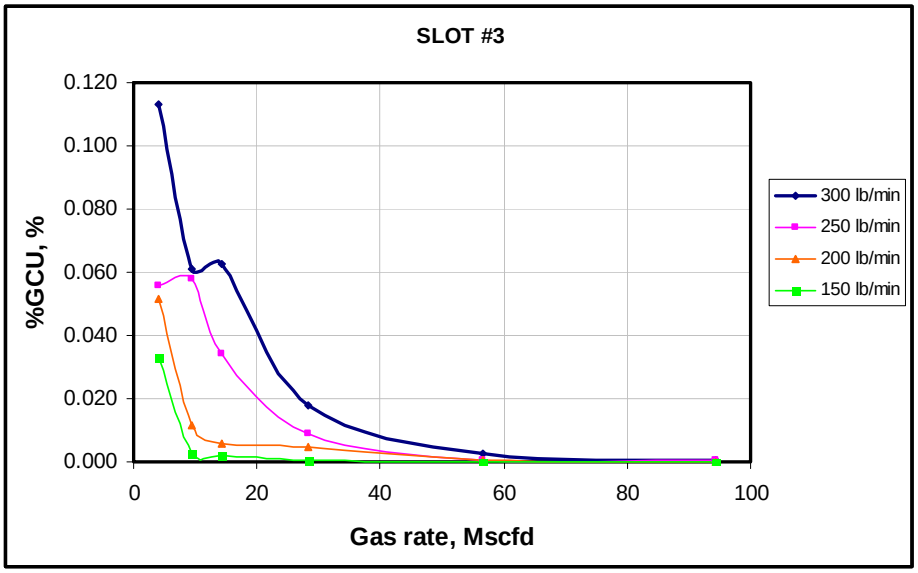

Fig. 5.6 Percent GCU trend for slot #3

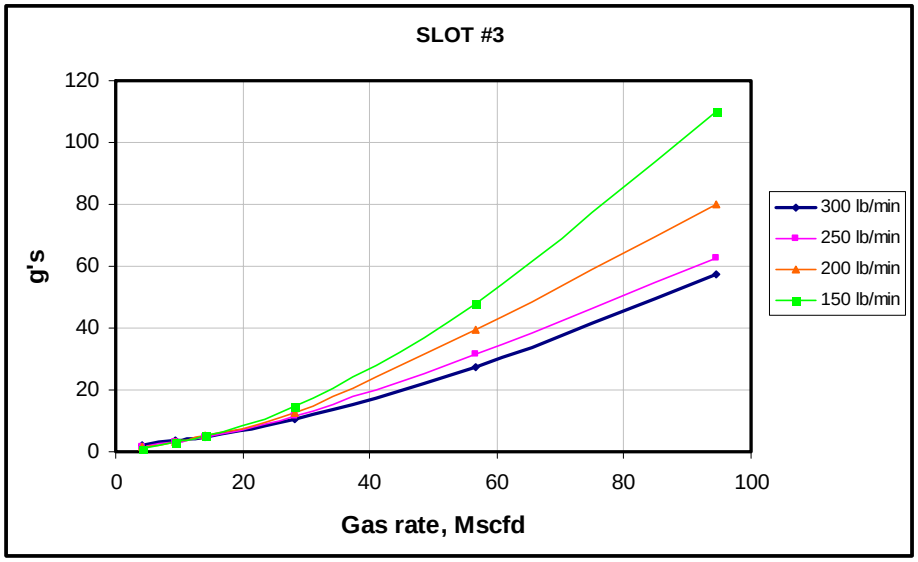

Fig. 5.7 g-force trend for slot #3

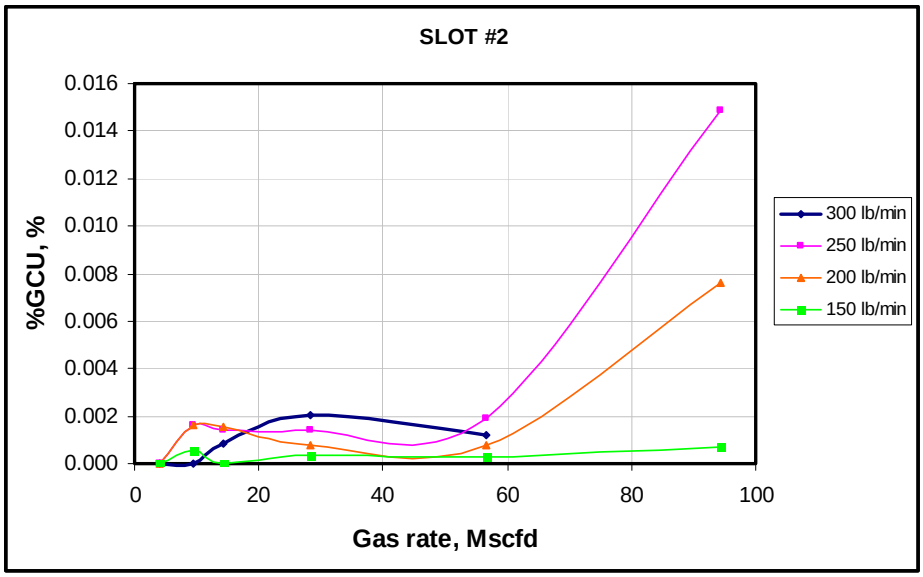

Fig. 5.8 Percent GCU trend for slot #2

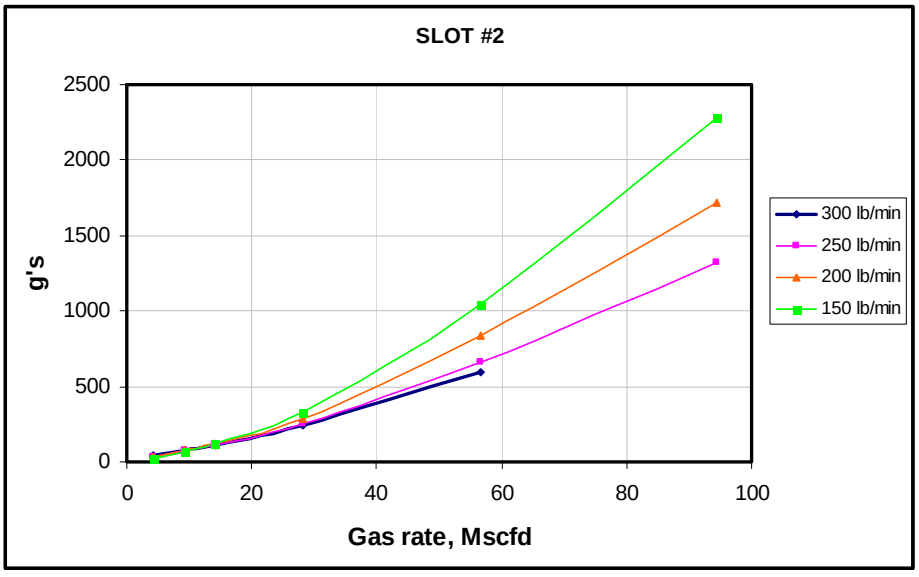

Fig. 5.9 g-force trend for slot #2

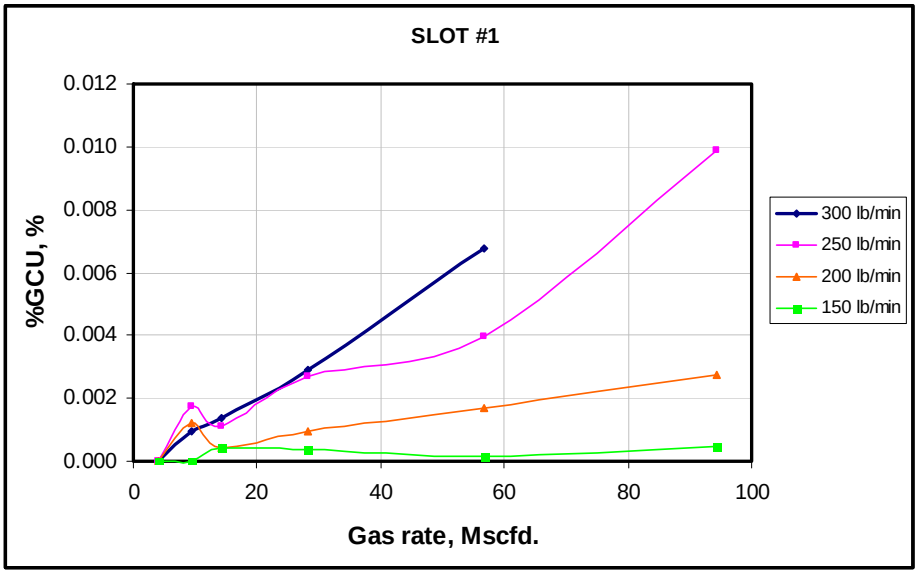

Fig. 5.10 Percent GCU trend for slot #1

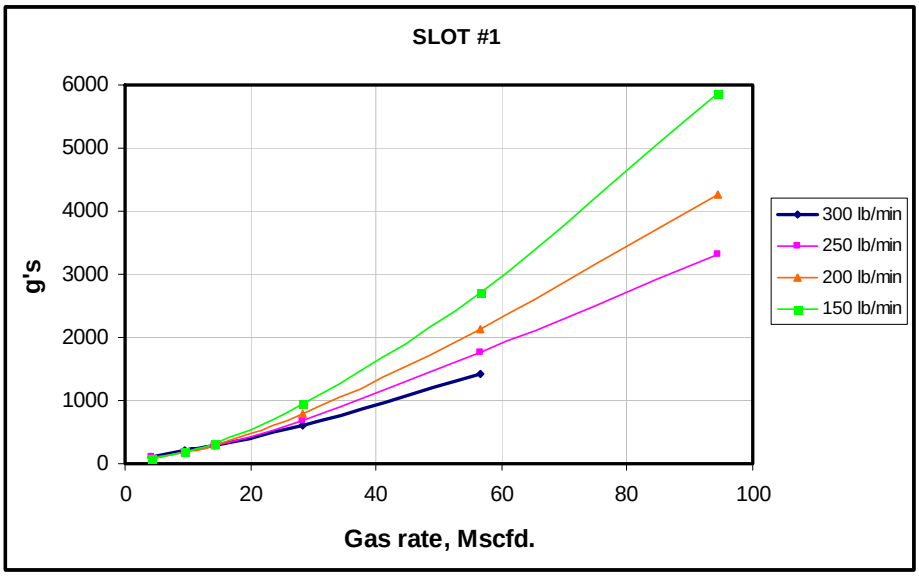

Fig. 5.11 g-force trend for slot #1

5.2.3 Improved GCU performance using step-wise change of inlet-slot size

For the GCU performance analysis of slots #1, #2 and #3, the percent GCU rate of all three slots have been plotted together for the 200- and 250-lb/min water rate cases. Also, the operating g's corresponding to these configurations are included in Fig. 5.12 and Fig. 5.13. The relevant sections of the previous percent GCU plots were "zoomed in".

Starting with the "250-lb/min"-trend (Fig. 5.12), we will start the GCU performance analysis from point 0 – the lowest gas rate. It is obvious for this operating condition the lowest GCU rate is achievable with slot #1. As the gas rate increases the separation g's increases for slot #1 along the curve *0 – 1-1*. At point 1, the GCU performance of slot #1 becomes poorer than that of slot #2. At this point, continued operation with slot #1 will result in greater gas carry-under due to excessive g's. For a fixed-slot configuration of a CCGL separator, this would imply operation along the line *0-1-4* (or *3-2-5* had we started the analysis from higher rates on slot #3). However, with a variable inlet-slot configuration, a step-wise change of slot size (*1-1 – 1-2*) to slot #2 would bring the g's back to about 140, thus improving the GCU performance along *1 – 2* (or *1-2 – 2-1* along the g's-curve). It should be noted here that although only three slot configurations were used in this investigation resulting in 600 g's being reached with slot #2, an intermediate slot would have been adequate for another down-stepping between points *2-1* and *2-2*. Notwithstanding, further changes in separator conditions in the form of increasing gas rates would require another step change in slot-size to slot #3 (*2-1 – 2-2* on g's-trend). This would further improve the GCU performance of the CCGL separator along the GCU performance trend *2 – 3*.

The same applies for the "200-lb/min"-trend in Fig. 5.13.

Thus, by using a variable-slot configuration in a CCGL separator, it is possible to expand the GCU operational envelope range as *qualitatively* demonstrated by the results of this experimental investigation. These results support the theoretical analysis presented earlier.

Based on the results and analysis of this investigation, the actual operational envelope expansion of a cylindrical cyclone gas/liquid separator by the use of changeable inlet-slots is in the *gas carry-under* performance and not in the *liquid carry-over*.

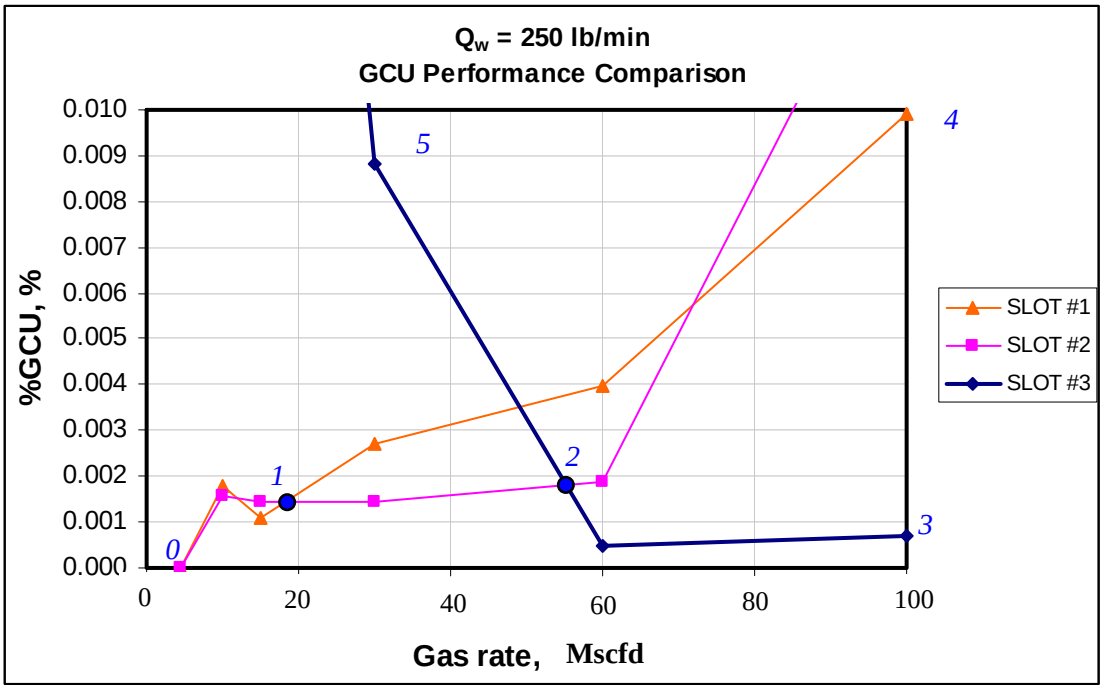

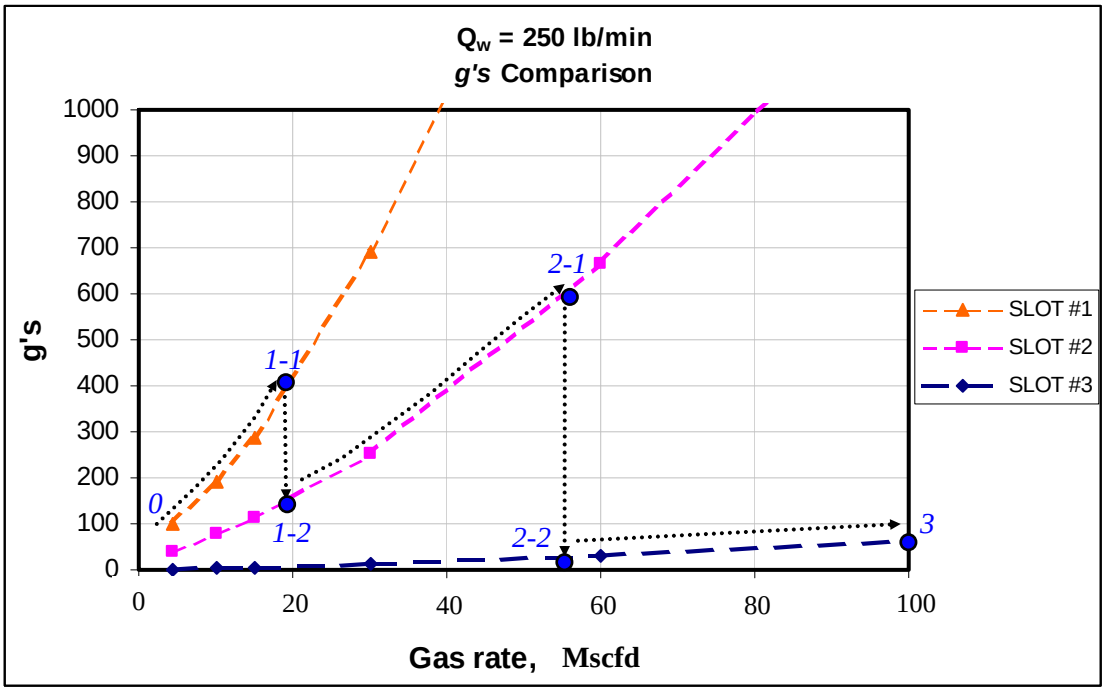

Fig. 5.12 GCU performance of slots #1-3 at 250-lb/min water rate

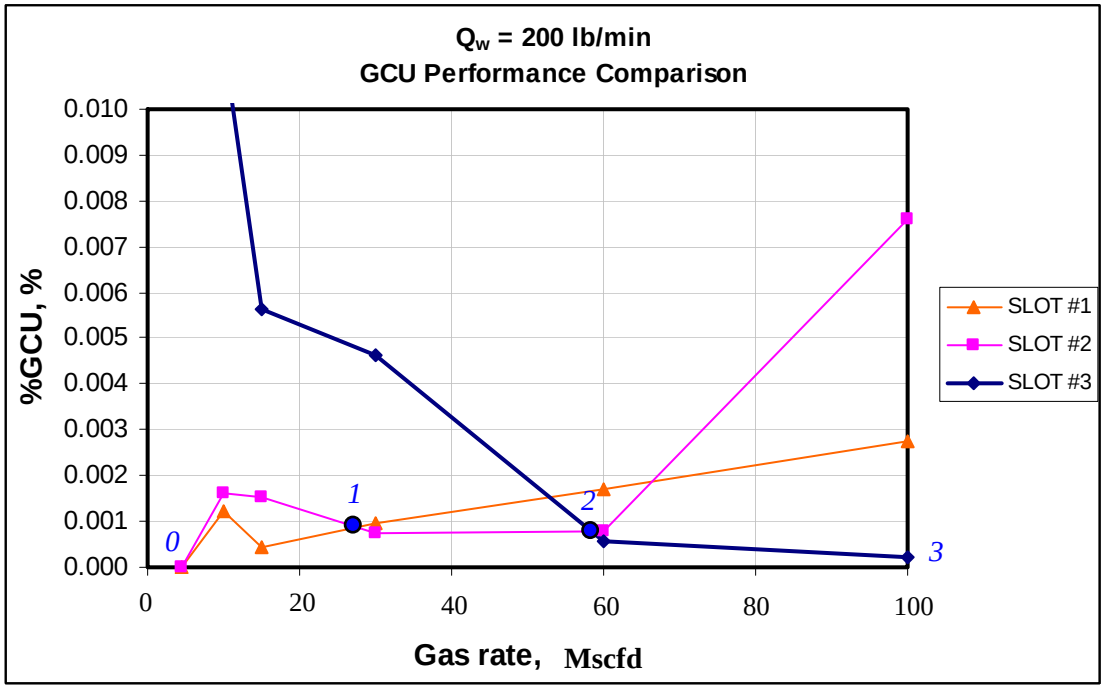

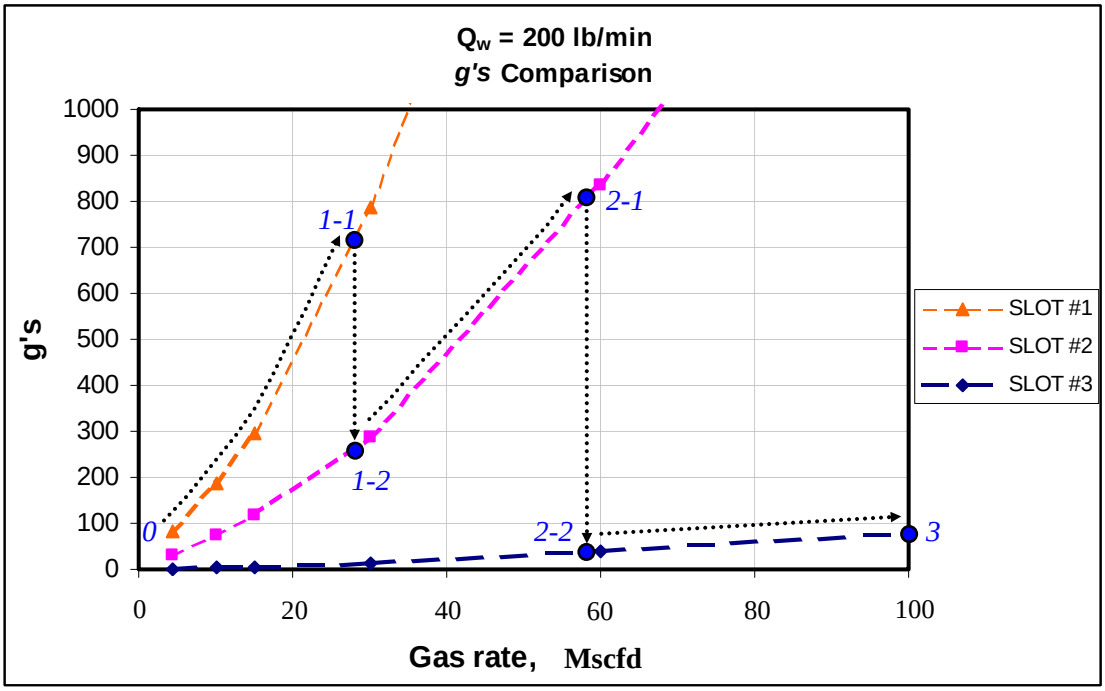

Fig. 5.13 GCU performance of slots #1-3 at 200-lb/min water rate

CHAPTER VI
CONCLUSIONS AND RECOMMENDATIONS

6.1 Conclusions

1. The actual area of possible operational envelope expansion of a cylindrical cyclone gas\liquid separator, by means of a variable inlet-slot configuration, is in the gas carry-under performance. The inlet-slot size variation has no noticeable effect or improvement on the liquid carry-over performance of the separator.
2. There is a good agreement between the theoretical analysis and experimental verification of the expanded GCU operational envelope achievable by the use of variable inlet-slots in a CCGL separator.
3. Expanding the liquid carry-over operational envelope can be achieved by operating the separator at higher pressures. Also, minimizing pressure losses in the liquid leg can improve the LCO operational envelope.
4. In a multiphase metering loop configuration of a CCGL separator, recombining the streams at the lowest possible point provides the best LCO operational envelope performance.
5. The ZNLF holdup is independent of the point of recombination of the gas and liquid phases.
6. Inlet slot-size has no effect on ZNLF holdup
7. The minimum g's required for efficient operation of a CCGL separator is in the 40 – 60 g's range.
8. Qualitatively, for an air – water system, separating environments in the 400 – 600 g's range and above worsens the GCU performance of the separator.

6.2 Recommendations

Based on the results obtained and findings of this experimental investigation, the following recommendation are made to improve on some of the data obtained, and ultimately, the conclusions reached:

1. Design of a more efficient gas-trap to improve on the GCU performance evaluation is necessary. A bigger (diameter-wise) gas-trap with a tangential inlet would improve on the GCU rate data. This would make possible, determining the upper-range value of g's necessary for separation and also include a quantitative dimension to the analysis.
2. Liquid carry-over tests at higher superficial gas and liquid velocities are needed to confirm that no noticeable operational envelope expansion is achieved by the use of a variable inlet-slot configuration in a CCGL separator.
3. More tests need to be run using other liquids such as crude oil to reveal any relationships, if it exists, between the g's required for efficient separation and fluid properties such as tendencies to foam.
4. A modular CCGL separator inlet-section with a variable inlet-slot configuration that allows automated or easy slot-size variation needs to be designed and tested on a field-scale basis at higher pressures.

NOMENCLATURE

A_{inlet} = inlet slot cross-sectional area

$A_{droplet}$ = liquid drop cross-sectional area

C_0 = flow coefficient

C_D = drag coefficient

D_l = liquid-leg internal diameter

d_{sep} = internal diameter of separator

$d_{droplet}$ *(microns),* $D_{droplet}$ = droplet diameter

f_{lH} = liquid frictional coefficient

F_{drag} , F_{bouy} = drag and buoyancy force respectively

g = acceleration due to gravity

GVF = gas volume fraction

H_L = liquid holdup

H_{LO} = ZNLF holdup

k = gas expansion/compression parameter

L_{eq} = equilibrium liquid level (ELL)

$L_{l\text{-}recomb}$ = distance between liquid-leg exit to recombination point

$L_{g\text{-}recomb}$ = distance between gas-leg exit to recombination point

L_{lH} = height of liquid in separator

L_{gH} = height of gas in separator

L_{gl} = length of separator gas-leg

L_d = droplet region length

m_{trap} = mass of trapped air

M_R = mass rate of trapped air

P = pressure

$P_{in\text{-}situ}$ = pressure of trapped air

Q_{t_insitu} = in-situ volumetric rate of trapped air

Q_{g_insitu} = in-situ gas volumetric flow rate

Q_g = gas volumetric flow rate

Q_l = liquid volumetric flow rate

Re = Reynold's number of separator

r_{sep} = radius of separator

t_{trap} = trap time

T = temperature

v_{SL} = superficial liquid velocity

v_{SG} = superficial gas velocity

v_{mr} = mixture velocity

v_s = slip velocity

v_G = gas velocity

v_{Go} = ZNLF gas velocity

v_{g_insitu} = in-situ gas velocity

v_L = liquid velocity

v_{lH} = axial liquid velocity in separator

V_t = terminal settling velocity

V_{trap} = volume of trapped air

α = angle of inclination of tangential inlet to the horizontal

ΣF_L = liquid frictional losses

ΣF_G = gas frictional losses

ρ_l = liquid density

ρ_g = gas density

σ = liquid surface tension

μ_g = gas viscosity

z = compressibility factor

%GCU = percent gas carry-under rate of inlet stream

REFERENCES

1. Barbuceanu, N. and Scott, S.: "Novel Inlet Design Expands Range of Operability for Compact Separator," paper SPE 71555 presented at the 2001 SPE Annual Technical Conference and Exhibition, New Orleans, September 30 – October 3.
2. Wang, S., Mohan, R., Shoham, O., Marrelli, J.D. and Kouba, G.E.: "Optimal Control Strategy and Experimental Investigation of Gas/Liquid Compact Separators," paper SPE 63120 presented at the 2000 SPE Annual Technical Conference and Exhibition, Dallas, October 1-4.
3. Millington, B.C. and Thew, M.T.: "LDA of Component Velocities in Air-water Models of Steam-water Cyclone Separators," *Proc.*, 3rd International Conference on Multphase Flow, The Hague, The Netherlands, (May 1987) 115-125.
4. Reydon, R.F. and Gauvin, W.H.: "Theoretical and Experimental Studies of Confined Vortex Flow," *The Canadian Journal of Chemical Engineering*, (February 1981) **59**, 14-23.
5. Bandyopadhyay, P.R., Pacifico, G.C. and Gad-el-Hak, M.: "Sensitivity of a Gas-Core Vortex in a Cyclone-Type Gas-Liquid Separator," Advanced Technology and Prototyping Division, Naval Undersea Warfare Center Division, Newport, Rhode Island, 1994.
6. Erdal, F., Shirazi, S., Shoham, O. and Kouba, G.: "CFD Simulation of Single-Phase and Two-Phase in Gas-Liquid Cylindrical Cyclone Separators," paper SPE 36645 presented at the 1996 SPE 71st Annual Meeting, Denver, October 6-9.
7. Kouba, G.E., Shoham, O. and Shirazi S.: "Design and Performance of Gas-Liquid Cylindrical Cyclone Separators," *Proc*., BHR Group 7th International Meeting on Multiphase Flow, Cannes, France, (1995) 307-327.
8. Marti, S., Erdal, F., Shoham, O. , Shirazi, S. and Kouba, G.: "Analysis of Gas Carry-Under in Gas/Liquid Cylindrical Cyclones," paper presented at the Hydrocyclones 1996 International Meeting, St. John College, Cambridge, England, April 2-4.
9. Arpandi I.A., Joshi A.R., Shoham, O., Shirazi, S. and Kouba, G.E.: "Hydrodynamics of Two-Phase Flow in Gas-Liquid Cylindrical Cyclone Separators," paper SPE 30683 presented at the 1995 SPE 70th Annual Meeting, Dallas, October 22-26.

10. Chirinos, W., Gomez, L., Wang, S., Mohan, R., Shoham, O. and Kouba, G.: "Liquid carry-over in Gas-Liquid Cylindrical Cyclone Compact Separators," paper presented at the 1999 SPE 74th Annual Meeting, Houston, October 3-6.
11. Gomez, L., Mohan, R., Shoham, O. and Kouba, G.: "Enhanced Mechanistic Model and Field Application Design of Gas-Liquid Cylindrical Cyclone Separator," paper SPE 49174 presented at the 1998 SPE 73rd Annual Meeting, New Orleans, September 27-30.
12. Isenberger, C.: "Design of a Novel Inlet for Compact Gas/Liquid Cylindrical Cyclone Separator Improves Separation," TAMU, Petroleum Department 7210 report, 1998.
13. Bill, N., Bentley, S. and Schwab, J.: "Compact Cyclone Multiphase Performance on The North Slope of Alaska," paper presented at 2002 Texas A&M Multiphase Measurement User Roundtable, May 8.
14. Bentley, N. S. and Kvamsdal, D.: "The Compact Cyclone Multiphase System," paper SPE 59711 presented at the 2000 SPE Permian Basin Oil and Gas Recovery Conference, Midland, Texas, March 21 –23.
15. Baker, A.C. and Entress, J. H.: "The VASPS Subsea Separation and Pumping System Applied to Marginal Field Developments," paper SPE 23049 presented at the 1991 Offshore Europe Conference, Aberdeen, September 3 – 6.
16. Weingarten, J.S.: "Field Results of Separations – Vessels and Multiphase-Flowline Debottlenecking Using An In-line Gas/Liquid Auger Separator," paper SPE 65072 presented at the 1998 SPE Annual Technical Conference and Exhibition, New Orleans, September.
17. Marrelli J.D. and Kouba, G.E.: "Methods for Optimal Matching of Separation and Metering Facilities for Performance, Cost, and Size: Practical Examples from Duri Area 10 Expansion," paper presented at the 2000 ETCE00-ER-10165, ETCE Conference of ASME Petroleum Division, New Orleans, February.
18. Duncan, R.W. and Scott, S.L.: "Vertical Zero Net Liquid Flow: Effects of High Pressure on Holdup," paper presented at the BHR Group Multiphase 1998 Conference, Banff, Canada, Vol. 31, 43 – 60.
19. Arnold, K. and Stewart, M.: "Surface Production Operations – Design of Oil-Handling Systems and Facilities (Vol.1)," 1986 by Gulf Publishing Company, Houston, Texas.
20. Kurokawa, J. and Ohtaki, T.: "Gas-Liquid Flow Characteristics and Gas-Separation Efficiency in a Cyclone Separator," *ASME FED Gas Liquid Flows*, (1995) **225**, 51-57.

21. Weingarten, J.S., Kolpak, M.M., Mattison, S.A. and Williamson, M.J.: "New Design for Compact Liquid-Gas Partial Separation: Downhole and Surface Installations for Artificial Lift Applications," paper SPE 30637 presented at the 1995 SPE 70th Annual Meeting, Dallas, Oct. 22-25.
22. Wolbert, D., Ma, B.F., Aurelle, Y. and Seureau, J.: "Efficiency Estimation of Liquid-Liquid Hydrocyclones Using Trajectory Analysis," *AIChe Journal*, (June 1995) **41**, No. 6 1395 – 1402.
23. Adejuyibe, B., Uvwo, I., Liu, J., Ejofodomi, O., Scott, S.L., Lansangan, R. and Dutton, R.: "Investigation of Three-Phase Flow Measurement Capabilities of a Coriolis Meter," paper presented at the 2004 BHRG Multiphase Conference, Banff, Canada, June 3 – 4.
24. Ayoub, J.A., Hill, A.D., Montgomery, C.T. and Scott, S.L.: "Production Operations from the Sandface to the Tanks," *SPE Journal of Petroleum Technology*, (July 2004), 36 – 39.
25. Gomez, L. E.: "Dispersed Two-Phase Swirling Flow Characterization For Predicting Gas Carry-Under in Gas-Liquid Cylindrical Cyclone Compact Separators," Ph. D. Dissertation, The University of Tulsa, 2001.
26. Turner, R.G., Hubbard, M.G. and Dukler, A.E., "Analysis and Prediction of Minimum Flow Rate for The Continuous Removal of Liquid from Gas Wells," *Journal of Petroleum Technology*, (March 1969) **21**, 1475 – 1482.
27. Hekimian, N., Jomonville, J.M. and Scott, S.L.: "Experimental Investigation of the Influence of Trace Amounts of Gas on Coriolis Liquid Metering," paper presented at the 2000 ASME-ETCE Production Technology Symposium, New Orleans, Louisiana, Feb. 14 – 17.
28. Gomez, L.E., Mohan, R., Shoham, O., Kouba, G., and Marrelli, J.D.: "State-of-the-Art Simulator for Field Applications of Gas Liquid Cylindrical Cyclone Separators," paper SPE 56581 presented at the 1999 SPE ATCE, Houston, Texas, October 3-6.

APPENDIX A

PERCENT GAS CARRY-UNDER EVALUATION ALGORITHM

Input data:

V_{trap} – volume of "trapped" air bubbles carried under, *ft^3*

t_{trap} – time duration for trapping V_{trap}, *seconds*

T – temperature of trapped air, *^oF*

P – pressure of trapped air, *psi*

Calculations:

Mass of air trapped, lb

$$m_{trap} = 2.6977 \cdot \frac{PV_{trap}}{T} \qquad \text{(A.1)}$$

Mass rate of trapped air, lb/sec.

$$M_R = \frac{m_{trap}}{t_{trap}} \qquad \text{(A.2)}$$

In-situ volumetric rate of trapped air, ft3/sec

$$Q_{t\_insitu} = 0.3707 \cdot M_R \cdot \frac{T}{P_{in-situ}} \qquad \text{(A.3)}$$

Flowing gas rate at in-situ conditions, ft3/sec

$$Q_{g\_insitu} = 0.3707 \cdot m_R \cdot \frac{T}{P_{in-situ}} \qquad \text{(A.4)}$$

Percent GCU rate, %

$$\%GCU = \frac{Q_{t\_insitu}}{Q_{g\_insitu}} \cdot 100 \qquad \text{(A.5)}$$

Gas volume fraction, %

$$GVF = \frac{Q_{t\_insitu}}{Q_{g\_insitu} + Q_l} \cdot 100 \qquad \text{(A.6)}$$

APPENDIX B

EXPERIMENTAL DATA SET

Table B.1 Zero-net liquid flow – slot #1-3

SLOT # 1				
Recombination #1				
	Qg	hL (measured)	hL (evaluated)	ZNLF hold-up
	ft3/sec	in.	in.	
1	0.053	36.00	35.46	0.739
2	0.077	24.00	25.20	0.525
3	0.089	23.00	23.94	0.499
4	0.121	18.50	19.86	0.414
5	0.168	15.00	15.70	0.327
6	0.233	11.50	11.55	0.241
7	0.445		5.57	0.116

SLOT # 2				
Recombination #1				
	Qg	hL (measured)	hL (evaluated)	ZNLF hold-up
	ft3/sec	in.	in.	
1	0.038	34.80	33.95	0.707
2	0.072	28.80	27.78	0.579
3	0.115	20.40	18.90	0.394
4	0.164	16.20	15.10	0.315
5	0.228	12.60	10.44	0.218
6	0.454	0.00	2.82	0.059

SLOT # 3				
Recombination #1				
	Qg	hL (measured)	hL (evaluated)	ZNLF hold-up
	ft3/sec	in.	in.	
1	0.037	0.00	34.11	0.711
2	0.068	0.00	25.84	0.538
3	0.115	23.00	19.45	0.405
4	0.160	18.50	17.16	0.357
5	0.220	15.00	12.35	0.257
6	0.455	11.50	4.60	0.096

Table B.2 Zero-net liquid flow – slot #1 (recombinations #1-3)

Recombination #1				
	Qg	hL (measured)	hL (evaluated)	ZNLF hold-up
	ft3/sec	in.	in.	
1	0.053	36.00	35.46	0.739
2	0.077	24.00	25.20	0.525
3	0.089	23.00	23.94	0.499
4	0.121	18.50	19.86	0.414
5	0.168	15.00	15.70	0.327
6	0.233	11.50	11.55	0.241
7	0.445		5.57	0.116

Recombination #2				
	Qg	hL (measured)	hL (evaluated)	ZNLF Hold-up
	ft3/sec	in.	in.	
1	0.042673	34.70	34.68	0.722
2	0.076968	26.00	25.69	0.535
3	0.122935	19.00	18.78	0.391
4	0.173031	15.00	15.37	0.320
5	0.235469	12.00	11.87	0.247
6	0.456961	5.00	4.37	0.091

Recombination #3				
	Qg	hL (measured)	hL (evaluated)	ZNLF Hold-up
	ft3/sec	in.	in.	
1	0.045	34.50	33.85	0.705
2	0.078	25.50	24.67	0.514
3	0.121	19.00	18.50	0.385
4	0.176	16.00	15.68	0.327
5	0.237	10.50	10.38	0.216
6	0.454	0.00	4.82	0.100

Table B.3 LCO operational envelope

Pressure 3 psi
SLOT # 1

	Recombination #1		Recombination #2		Recombination #3	
	VsL	Vsg	VsL	Vsg	VsL	Vsg
	ft/sec					
1	0.995	0.715	0.942	0.682	0.896	0.758
2	0.949	1.428	0.903	1.479	0.855	1.488
3	0.904	2.400	0.824	2.589	0.753	2.688
4	0.815	3.699	0.806	3.519	0.711	3.738
5	0.764	5.473	0.725	5.327	0.621	5.519
6	0.736	7.176	0.715	7.061	0.568	7.328
7	0.648	10.642	0.572	11.183	0.488	11.346
8	0.585	14.672	0.559	14.081	0.468	14.340
9	0.522	18.157	0.529	17.815	0.467	17.707

Table B.4 LCO operational envelope – separator pressure

Pressure 9 psi
Recomb 1

	SLOT #1		SLOT #2		SLOT #3	
	VsL	Vsg	VsL	Vsg	VsL	Vsg
	ft/sec					
1	0.812	14.655	1.478	0.617	0.868	14.293
2	0.913	11.526	1.425	1.189	0.943	11.426
3	1.042	8.268	1.324	2.141	1.026	8.480
4	1.134	5.508	1.284	2.828	1.164	5.570
5	1.298	2.751	1.129	5.757	1.303	2.898
6	1.357	1.981	0.989	8.847	1.342	2.042
7	1.348	1.188	0.933	11.455	1.442	1.124
8	1.466	0.578	0.861	14.141	1.483	0.574

Pressure 3 psi
Recomb 1

	SLOT #1		SLOT #2		SLOT #3	
	VsL	Vsg	VsL	Vsg	VsL	Vsg
	ft/sec					
1	0.585	14.672	0.904	0.797	0.977	0.773
2	0.522	18.157	0.955	1.547	0.902	1.499
3	0.648	10.642	0.820	2.746	0.858	2.645
4	0.653	7.297	0.827	3.604	0.843	3.581
5	0.785	3.572	0.703	7.520	0.715	7.346
6	0.852	2.556	0.630	11.054	0.619	11.234
7	0.934	1.480	0.623	13.999	0.611	14.670
8	0.937	0.754	0.587	18.195	0.586	17.914

Pressure 6 psi
Recomb 1

	SLOT #1		SLOT #2		SLOT #3	
	VsL	Vsg	VsL	Vsg	VsL	Vsg
	ft/sec					
1	1.244	0.660	1.232	0.665	1.217	0.724
2	1.176	1.327	1.177	1.392	1.187	1.354
3	1.098	2.340	1.099	2.443	1.113	2.320
4	1.007	3.299	1.036	3.440	1.070	3.168
5	0.903	6.508	0.909	6.587	0.964	6.311
6	0.858	9.461	0.835	9.673	0.864	9.680
7	0.781	12.624	0.772	12.616	0.805	12.609
8	0.730	15.564	0.696	15.912	0.752	15.446

Table B.5 GCU operational envelope – slot #1 (constant gas rate)

Gas rate, lb/min			MFR_W	Vsl	Vsg	P_sep	%GCU	GVF	g's
			lb/min	ft/sec	ft/sec	psi	%	%	_
0.22		300	291.3418	1.588808	0.550128	12	0	0	115.77
		250	248.4238	1.354756	0.652089	9	0	0	101.89
		200	200.9479	1.096347	0.730302	6	0	0	84.40
		150	151.387	0.826141	0.843389	3	0	0	70.48
									93.14

Gas rate, lb/min			MFR_W	Vsl	Vsg	P_sep	%GCU	GVF	g's
			lb/min	ft/sec	ft/sec	psi	%	%	_
0.5		300	311.5324	1.698552	1.152971	13.5	0.00093235	0.000618	205.70
		250	247.1736	1.347861	1.417375	10	0.001770421	0.001808	193.32
		200	200.0638	1.091297	1.6427	6	0.001229012	0.00178	188.93
		150	150.3768	0.820381	1.86457	3	0	0	182.15
									192.53

Gas rate, lb/min			MFR_W	Vsl	Vsg	P_sep	%GCU	GVF	g's
			lb/min	ft/sec	ft/sec	psi	%	%	_
0.75		300	289.5923	1.578496	1.783301	14	0.001370668	0.001508	285.71
		250	249.1581	1.357784	2.008594	10	0.001109971	0.001594	286.44
		200	200.2687	1.091473	2.324098	6	0.000444056	0.000907	294.81
		150	151.1949	0.824085	2.703786	3	0.000436437	0.001375	314.41
									295.34

Gas rate, lb/min			MFR_W	Vsl	Vsg	P_sep	%GCU	GVF	g's
			lb/min	ft/sec	ft/sec	psi	%	%	_
1.5		300	305.3465	1.664934	3.262776	16.5	0.002901715	0.005573	613.75
		250	249.4993	1.359921	3.874943	12.5	0.00272243	0.007559	692.50
		200	200.5689	1.093349	4.492286	8	0.00095522	0.003798	788.51
		150	150.5356	0.820796	5.263119	4	0.000347235	0.00215	935.62
									757.59

Gas rate, lb/min			MFR_W	Vsl	Vsg	P_sep	%GCU	GVF	g's
			lb/min	ft/sec	ft/sec	psi	%	%	_
3.0		300	305.0809	1.663296	5.84884	20	0.006779942	0.023538	1426.18
		250	247.5475	1.350469	6.992569	14	0.003964526	0.020105	1758.55
		200	200.254	1.092682	8.094997	10	0.00168845	0.012203	2133.14
		150	150.2891	0.82018	9.551132	6.5	0.00016068	0.001812	2719.12
									2009.25

Gas rate, lb/min			MFR_W	Vsl	Vsg	P_sep	%GCU	GVF	g's
			lb/min	ft/sec	ft/sec	psi	%	%	_
5.0		300							
		250	245.9029	1.341174	10.11454	18	0.009910283	0.073804	3315.82
		200	201.4811	1.098775	11.89686	13	0.002743634	0.029031	4270.36
		150	149.6662	0.816495	14.40312	7	0.000463516	0.007995	5858.67
									4481.62

Table B.6 GCU operational envelope – slot #1 (constant liquid rate)

Gas Rate		300 lb/min					
lb/min	cfd	**Vsl**	**Vsg**	**P_sep**	**%GCU**	**GVF**	**g's**
0.22	4,154	1.588808	0.550128	12	0	0	115.77
0.50	9,441	1.698552	1.698552	13.5	0.00093235	0.000618	205.70
0.75	14,162	1.578496	1.783301	14	0.001370668	0.001508	285.71
1.50	28,324	1.664934	3.262776	16.5	0.002901715	0.005573	613.75
3.00	56,648	1.663296	5.84884	20	0.006779942	0.023538	1426.18
5.00	94,413						

Gas Rate		250 lb/min					
lb/min	cfd	**Vsl**	**Vsg**	**P_sep**	**%GCU**	**GVF**	**g's**
0.22	4,154	1.354756	0.652089	9	0	0	101.89
0.50	9,441	1.347861	1.417375	10	0.001770421	0.001808	193.32
0.75	14,162	1.357784	2.008594	10	0.001109971	0.001594	286.44
1.50	28,324	1.359921	3.874943	12.5	0.00272243	0.007559	692.50
3.00	56,648	1.350469	6.992569	14	0.003964526	0.020105	1758.55
5.00	94,413	1.341174	10.11454	18	0.009910283	0.073804	3315.82

Gas Rate		200 lb/min					
lb/min	cfd	**Vsl**	**Vsg**	**P_sep**	**%GCU**	**GVF**	**g's**
0.22	4,154	1.096347	0.730302	6	0	0	84.40
0.50	9,441	1.091297	1.6427	6	0.001229012	0.00178	188.93
0.75	14,162	1.091473	2.324098	6	0.000444056	0.000907	294.81
1.50	28,324	1.093349	4.492286	8	0.00095522	0.003798	788.51
3.00	56,648	1.092682	8.094997	10	0.00168845	0.012203	2133.14
5.00	94,413	1.098775	11.89686	13	0.002743634	0.029031	4270.36

Gas Rate		150 lb/min					
lb/min	cfd	**Vsl**	**Vsg**	**P_sep**	**%GCU**	**GVF**	**g's**
0.22	4,154	0.826141	0.843389	3	0	0	70.48
0.50	9,441	0.820381	1.86457	3	0	0	182.15
0.75	14,162	0.824085	2.703786	3	0.000436437	0.001375	314.41
1.50	28,324	0.820796	5.263119	4	0.000347235	0.00215	935.62
3.00	56,648	0.82018	9.551132	6.5	0.00016068	0.001812	2719.12
5.00	94,413	0.816495	14.40312	7	0.000463516	0.007995	5858.67

Table B.7 GCU operational envelope – slot #2 (constant gas rate)

Gas rate, lb/min			MFR_W	Vsl	Vsg	P_sep	%GCU	GVF	g's
			lb/min	ft/sec	ft/sec	psi	%	%	_
0.22		300	301.4806	1.645441	0.535347	12	0	0	47.02
		250	251.0165	1.370005	0.603022	9	0	0	38.48
		200	201.9107	1.10204	0.711442	5	0	0	32.50
		150	151.6878	0.827928	0.807667	3	0	0	26.43
									36.11

Gas rate, lb/min			MFR_W	Vsl	Vsg	P_sep	%GCU	GVF	g's
			lb/min	ft/sec	ft/sec	psi	%	%	_
0.5		300	299.0122	1.630507	1.194416	14	0	0	78.84
		250	251.8397	1.373536	1.419116	10	0.00158754	0.001577	77.03
		200	202.6225	1.105352	1.650133	6	0.001608928	0.002298	74.96
		150	150.7603	0.822117	1.844791	3	0.000580367	0.00124	70.20
									75.26

Gas rate, lb/min			MFR_W	Vsl	Vsg	P_sep	%GCU	GVF	g's
			lb/min	ft/sec	ft/sec	psi	%	%	_
0.75		300	300.852	1.640835	1.764907	14	0.000829904	0.000862	114.55
		250	250.0133	1.362902	2.036327	10	0.001424319	0.002053	114.08
		200	200.5439	1.093646	2.382323	7	0.001515997	0.003167	119.26
		150	150.9946	0.823355	2.728019	3	0	0	124.47
									118.09

Gas rate, lb/min			MFR_W	Vsl	Vsg	P_sep	%GCU	GVF	g's
			lb/min	ft/sec	ft/sec	psi	%	%	_
1.5		300	299.4123	1.633177	3.289321	16.5	0.002066935	0.004058	239.19
		250	252.0817	1.375101	3.694888	12	0.001443869	0.003764	253.70
		200	200.3564	1.092606	4.311606	8.5	0.000748038	0.002855	288.23
		150	150.9971	0.823446	4.987856	4.5	0.000350823	0.002043	333.37
									278.62

Gas rate, lb/min			MFR_W	Vsl	Vsg	P_sep	%GCU	GVF	g's
			lb/min	ft/sec	ft/sec	psi	%	%	_
3.0		300	298.5391	1.62799	6.135017	18	0.001184538	0.00437	594.64
		250	250.8916	1.367818	6.847722	15	0.001874123	0.009192	665.97
		200	200.3929	1.092621	8.114346	10	0.000790863	0.005689	836.49
		150	154.0718	0.84023	9.471925	7	0.000311117	0.003387	1049.57
									786.67

Gas rate, lb/min			MFR_W	Vsl	Vsg	P_sep	%GCU	GVF	g's
			lb/min	ft/sec	ft/sec	psi	%	%	_
5.0		300							
		250	247.6505	1.349131	10.20204	18	0.014855372	0.108803	1316.49
		200	200.7744	1.094087	12.11429	13	0.007617669	0.082469	1721.50
		150	151.9413	0.827951	14.37884	9	0.000675541	0.011381	2282.46
									1773.48

Table B.8 GCU operational envelope – slot #2 (constant liquid rate)

Gas Rate		300 lb/min					
lb/min	cfd	**Vsl**	**Vsg**	**P_sep**	**%GCU**	**GVF**	**g's**
0.22	4,154	1.645441	0.535347	12	0	0	47.02
0.50	9,441	1.630507	1.630507	14	0	0	78.84
0.75	14,162	1.640835	1.764907	14	0.000829904	0.000862	114.55
1.50	28,324	1.633177	3.289321	16.5	0.002066935	0.004058	239.19
3.00	56,648	1.62799	6.135017	18	0.001184538	0.00437	594.64
5.00							

Gas Rate		250 lb/min					
lb/min	cfd	**Vsl**	**Vsg**	**P_sep**	**%GCU**	**GVF**	**g's**
0.22	4,154	1.370005	0.603022	9	0	0	38.48
0.50	9,441	1.373536	1.419116	10	0.00158754	0.001577	77.03
0.75	14,162	1.362902	2.036327	10	0.001424319	0.002053	114.08
1.50	28,324	1.375101	3.694888	12	0.001443869	0.003764	253.70
3.00	56,648	1.367818	6.847722	15	0.001874123	0.009192	665.97
5.00	94,413	1.349131	10.20204	18	0.014855372	0.108803	1316.49

Gas Rate		200 lb/min					
lb/min	cfd	**Vsl**	**Vsg**	**P_sep**	**%GCU**	**GVF**	**g's**
0.22	4,154	1.10204	0.711442	5	0	0	32.50
0.50	9,441	1.105352	1.650133	6	0.001608928	0.002298	74.96
0.75	14,162	1.093646	2.382323	7	0.001515997	0.003167	119.26
1.50	28,324	1.092606	4.311606	8.5	0.000748038	0.002855	288.23
3.00	56,648	1.092621	8.114346	10	0.000790863	0.005689	836.49
5.00	94,413	1.094087	12.11429	13	0.007617669	0.082469	1721.50

Gas Rate		150 lb/min					
lb/min	cfd	**Vsl**	**Vsg**	**P_sep**	**%GCU**	**GVF**	**g's**
0.22	4,154	0.827928	0.807667	3	0	0	26.43
0.50	9,441	0.822117	1.844791	3	0.000580367	0.00124	70.20
0.75	14,162	0.823355	2.728019	3	0	0	124.47
1.50	28,324	0.823446	4.987856	4.5	0.000350823	0.002043	333.37
3.00	56,648	0.84023	9.471925	7	0.000311117	0.003387	1049.57
5.00	94,413	0.827951	14.37884	9	0.000675541	0.011381	2282.46

Table B.9 GCU operational envelope – slot #3 (constant gas rate)

Gas rate, lb/min			MFR_W	Vsl	Vsg	P_sep	%GCU	GVF	g's
			lb/min	ft/sec	ft/sec	psi	%	%	_
0.22		300	302.5375	1.649736	0.56117	12	0.113354223	0.036538	2.09
		250	253.6405	1.383146	0.645495	9	0.055842503	0.024702	1.76
		200	202.1725	1.102457	0.741492	5	0.051819388	0.032935	1.45
		150	154.8745	0.844584	0.832139	3	0.033008108	0.030691	1.20
									1.62

Gas rate, lb/min			MFR_W	Vsl	Vsg	P_sep	%GCU	GVF	g's
			lb/min	ft/sec	ft/sec	psi	%	%	_
0.5		300	305.2729	1.664054	1.23051	13.5	0.060924124	0.042545	3.57
		250	258.1292	1.407373	1.38305	10	0.057722655	0.053637	3.32
		200	208.7309	1.138114	1.576165	6	0.011441193	0.015029	3.14
		150	152.5194	0.831574	1.853091	3	0.002390218	0.005041	3.07
									3.28

Gas rate, lb/min			MFR_W	Vsl	Vsg	P_sep	%GCU	GVF	g's
			lb/min	ft/sec	ft/sec	psi	%	%	_
0.75		300	305.0534	1.662693	1.750541	14	0.062395533	0.062112	4.97
		250	255.7491	1.394172	2.021003	10	0.033950918	0.046317	4.97
		200	204.6102	1.115464	2.314044	6.5	0.005615093	0.01108	5.01
		150	146.3131	0.797749	2.747022	3	0.002134123	0.006906	5.35
									5.08

Gas rate, lb/min			MFR_W	Vsl	Vsg	P_sep	%GCU	GVF	g's
			lb/min	ft/sec	ft/sec	psi	%	%	_
1.5		300	305.6717	1.666141	3.269131	16	0.017688823	0.033074	10.38
		250	256.7772	1.39969	3.777662	12	0.008807675	0.022616	11.42
		200	209.0696	1.139682	4.327862	8	0.004627189	0.016779	12.74
		150	156.8667	0.855118	5.068809	4	0.000542056	0.00305	14.95
									12.37

Gas rate, lb/min			MFR_W	Vsl	Vsg	P_sep	%GCU	GVF	g's
			lb/min	ft/sec	ft/sec	psi	%	%	_
3.0		300	285.044	1.553318	6.446314	18	0.002727123	0.010929	27.26
		250	251.9754	1.373155	7.211755	14	0.000496027	0.00251	31.42
		200	201.4286	1.097545	8.51046	9	0.000558598	0.004157	39.33
		150	151.2935	0.824384	9.794132	6	0.000259166	0.002956	48.04
									36.51

Gas rate, lb/min			MFR_W	Vsl	Vsg	P_sep	%GCU	GVF	g's
			lb/min	ft/sec	ft/sec	psi	%	%	_
5.0		300	263.7088	1.437097	10.17175	19	0.000679435	0.00467	57.40
		250	248.0922	1.352016	10.76247	17.5	0.000679147	0.005254	62.52
		200	203.5156	1.109234	12.59552	13	0.000198424	0.000198	80.01
		150	151.7083	0.826756	15.25114	8	9.92745E-05	0.001762	110.16
									77.52

Table B.10 GCU operational envelope – slot #3 (constant liquid rate)

Gas Rate		300 lb/min					
lb/min	cfd	**Vsl**	**Vsg**	**P_sep**	**%GCU**	**GVF**	**g's**
0.22	4,154	1.649736	0.56117	12	0.113354223	0.036538	2.09
0.50	9,441	1.664054	1.664054	13.5	0.060924124	0.042545	3.57
0.75	14,162	1.662693	1.750541	14	0.062395533	0.062112	4.97
1.50	28,324	1.666141	3.269131	16	0.017688823	0.033074	10.38
3.00	56,648	1.553318	6.446314	18	0.002727123	0.010929	27.26
5.00	94,413	1.437097	10.17175	19	0.000679435	0.00467	57.40

Gas Rate		250 lb/min					
lb/min	cfd	**Vsl**	**Vsg**	**P_sep**	**%GCU**	**GVF**	**g's**
0.22	4,154	1.383146	0.645495	9	0.055842503	0.024702	1.76
0.50	9,441	1.407373	1.38305	10	0.057722655	0.053637	3.32
0.75	14,162	1.394172	2.021003	10	0.033950918	0.046317	4.97
1.50	28,324	1.39969	3.777662	12	0.008807675	0.022616	11.42
3.00	56,648	1.373155	7.211755	14	0.000496027	0.00251	31.42
5.00	94,413	1.352016	10.76247	17.5	0.000679147	0.005254	62.52

Gas Rate		200 lb/min					
lb/min	cfd	**Vsl**	**Vsg**	**P_sep**	**%GCU**	**GVF**	**g's**
0.22	4,154	1.102457	0.741492	5	0.051819388	0.032935	1.45
0.50	9,441	1.138114	1.576165	6	0.011441193	0.015029	3.14
0.75	14,162	1.115464	2.314044	6.5	0.005615093	0.01108	5.01
1.50	28,324	1.139682	4.327862	8	0.004627189	0.016779	12.74
3.00	56,648	1.097545	8.51046	9	0.000558598	0.004157	39.33
5.00	94,413	1.109234	12.59552	13	0.000198424	0.000198	80.01

Gas Rate		150 lb/min					
lb/min	cfd	**Vsl**	**Vsg**	**P_sep**	**%GCU**	**GVF**	**g's**
0.22	4,154	0.844584	0.832139	3	0.033008108	0.030691	1.20
0.50	9,441	0.831574	1.853091	3	0.002390218	0.005041	3.07
0.75	14,162	0.797749	2.747022	3	0.002134123	0.006906	5.35
1.50	28,324	0.855118	5.068809	4	0.000542056	0.00305	14.95
3.00	56,648	0.824384	9.794132	6	0.000259166	0.002956	48.04
5.00	94,413	0.826756	15.25114	8	9.92745E-05	0.001762	110.16

APPENDIX C

CCGL SEPARATOR TEST SECTION

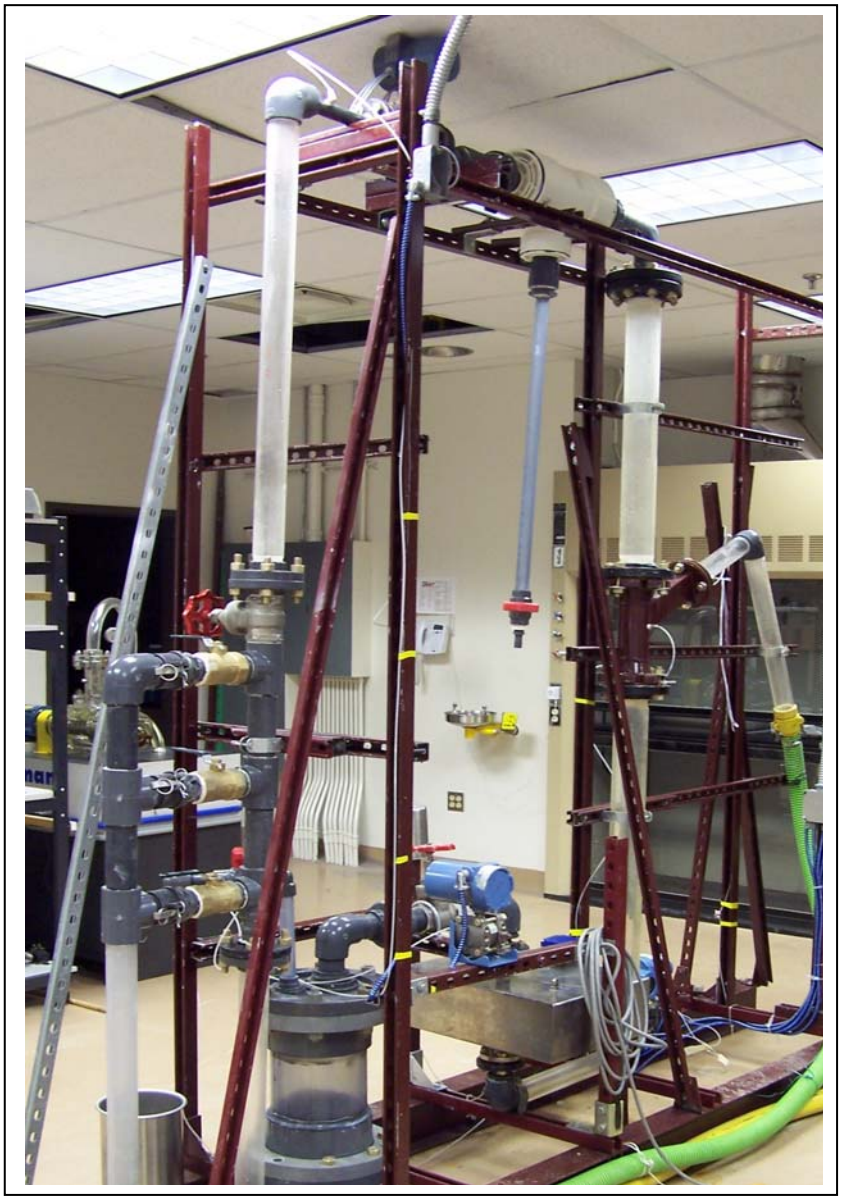

Fig. C.1 Experimental setup of CCGL separator in metering loop configuration

Fig. C.2 Gas core filament as viewed in CCGL separator while in operation

Fig. C.3 Inlet-section and insert spool

Fig. C.4 Insert spools #1 and #2

VITA

Ighofasan Uvwo completed his Bachelor of Engineering degree in Technological Machines and Equipment for Oil and Gas Fields at the Russian State Oil and Gas University, Moscow, Russia in June 2002. His permanent address is 7311 Eden Crossing Lane, Richmond, TX 77469.